This is a peer-reviewed, accepted author manuscript of the following research article: de Jonge-Anderson, I & Underhill, JR 2020, 'Structural constraints on Lower Carboniferous shale gas exploration in the Craven Basin, NW England', Petroleum Geoscience, vol. 26, no. 2, pp. 303-324. https://doi.org/10.1144/petgeo2019-125

Structural constraints on Lower Carboniferous shale gas exploration in the Craven Basin, NW England

Iain Anderson*& John R. Underhill

Institute of GeoEnergy Engineering (IGE), School of Energy, Geoscience, Infrastructure & Society, Heriot-Watt University, Edinburgh, EH14 4AS, UK

Corresponding author (email: ia205@hw.ac.uk)

Abstract: Seismic interpretation of a 3D seismic volume reveals the detrimental effect that post-depositional tectonic deformation has had on buried Lower Carboniferous (Dinantian-Namurian) shales and its consequence for shale gas prospectivity in the SW part (Fylde area) of the Craven Basin in NW England. The structural styles primarily result from Devono-Carboniferous (syn-sedimentary) extension, post-rift subsidence and Variscan inversion, a renewed phase of Permo-Triassic extension and Cenozoic uplift and basin exhumation. In contrast to the shallow dips and bedding continuity that characterizes productive shale gas plays in other basins (e.g. in the USA and Argentina), our mapping shows that the area is affected by deformation events that result in Bowland Shale Formation targets being folded and dissected into fault-bound compartments defined by SW-NE (Lower Carboniferous & Variscan) reverse faults and SSW-NNE to N-S (Permo-Triassic) normal faults. The fault networks and the misalignment between the elongate compartments they contain and the present-day minimum horizontal stress orientation limit the length over which long, lateral boreholes can remain in a productive horizon; placing an important constraint on optimal well positioning, reducing the size of resource and affecting well productivity. Our

subsurface mapping using this high-fidelity dataset provides an accurate picture of the subsurface structure that has direct and significant consequences for: the location of well pads; the lateral continuity of target shale gas horizons; the evaluation of the risk of inducing seismicity on seismically resolvable (large displacement) fault planes prior to drilling: and the likelihood of faults with small throws (below seismic resolution) being present.

Introduction and Rationale

Unconventional shale plays have revolutionised the petroleum industry in the US to the extent that the country has reverted to being self-sufficient for its energy needs and become a net gas exporter for the first time in over half a century. Founded on that exploration success, other plays have been investigated around the world, but with a varying degree of success. Selley (2005) suggested that there was shale gas potential in the UK and a number of basins were subsequently screened by Smith *et al* (2010).

While the Jurassic of the Weald Basin and Lower Carboniferous (West Lothian Oil Shale Group) in the Midland Valley of Scotland provided some encouragement, Smith et al (2010) suggested that the Carboniferous (Visean-Namurian) deep-water sediments ascribed to the Bowland and Hodder shales in the Craven Basin, Edale Basin, Widmerpool Gulf, Gainsborough Trough and Cleveland Basin of Northern England (Fig.1) were especially prospective. Subsequent studies have served to underline the potential (Roche 2012; Andrews 2013; Slowakiewicz *et al.* 2015; Yang et al., 2015; Könitzer *et al.*, 2016; Hennissen *et al.* 2017; Harvey *et al.* 2018; Hughes *et al.* 2018; Newport *et al.*, 2018) and extend the opportunity to include parts of North Wales too, where the corresponding units are known as the Holywell Shale Formation (Newport *et al.,* 2016).

The shale gas potential that was recognised by the aforementioned regional studies led to a renewed exploration interest in the Carboniferous basins and a number of Petroleum Exploration and Development Licenses (PEDL) were bid for, and subsequently awarded, in the 13th and 14th Onshore Licensing Rounds in 2011 and 2015. Initial resource estimates for all of the main plays were published in 2013-14 and suggested that the UK's shale resources were large (Andrews 2013, 2014; Monaghan 2014). Collectively, the studies acted as a catalyst for renewed industry activity and promoted the notion that shale gas resources could be sufficient to help wean the country off its increasing dependency on petroleum imports (Harvey *et al.* 2018).

The aim of the paper is to present the results of an independent evaluation of the subsurface geology in a strategic part of the PEDL 165 license in the Fylde area, NW Lancashire. The license is situated in the south-westerly extension of the Craven Basin, where it is buried beneath a Permo-Triassic sedimentary cover (Fig.2), which was identified as a prime candidate for shale gas extraction and where exploration drilling activity has already taken place (Clarke *et al.* 2018). Important new insights regarding the subsurface stratigraphy and structure of the area have emerged from our mapping including the role of Permo-Triassic extension and the severity of Late Carboniferous (Variscan) fold-and-fault deformation and their effect on shale gas targets. The results have direct implications for unconventional shale gas exploration in the PEDL 165 license since the deformation compartmentalises and limits the play and impacts resource estimates. The identification of fault networks also poses further challenges as demonstrated by human-induced seismicity during hydraulic fracturing operations at two drill sites (Preese Hall-1 and Preston New Road (PNR); Clarke *et al.* 2014, 2019).

Regional Setting

The 3D data volume was acquired in 2012 over an area where Permian and Triassic clastic red beds outcrop (Fig. 2), the occurrence of which represents the onshore expression of the East Irish Sea Basin (EISB). The basal sequences extend east and have an unconformable or faulted contact with truncated Carboniferous sediments belonging to the SW-NE striking Craven Basin (Figs.1-2). The basin is one of a number of Late Devonian to Carboniferous (Mississippian) depocentres that formed in response to N-S to NW-SE oriented rifting (Fig.1), the orientation of which appears to have been largely governed by the reactivation of Caledonian structures (Leeder 1982; Fraser & Gawthorpe, 1990 & 2003; Fraser *et al.*, 1990; Corfield *et al.* 1996; Glennie & Underhill 1998; Worthington & Walsh 2011).

The Craven Basin underwent a phase of (post-rift) thermal subsidence during the Namurian and Westphalian (Pennsylvanian) before being affected by foreland deformation associated with the Variscan Orogeny to the south (Glennie & Underhill 1998). The main zone of deformation is known as the Ribblesdale Fold Belt and consists of a suite of largely SW-NE striking, *en echelon* folds and reverse faults (Arthurton *et al.* 1988) that collectively plunge beneath the Permo-Triassic succession to the south-west (Fig.2). The SE margin of the fold belt is marked by the Pendle Monocline, which effectively separates the Craven Basin from the West Lancashire High and represents the surface expression of a reactivated (structurally inverted), NW-dipping planar normal fault (Chadwick & Evans 2005). Its north-western margin counterpart separates the basin from the Lancaster High (Lawrence *et al.* 1987) and is marked by a SE-dipping (antithetic) fault against which a series of oblique folds occur (e.g. the Sykes and Catlow Anticlines etc (Moseley 1962; Arthurton 1984; Kirby *et al.* 2000; Fig. 2). A recent study by Pharoah et al. (2019) has also suggested that the fold belt extends across southern parts of the EISB to affect parts of NW Wales including Anglesey and called it the Môn-Deemster fold-and-thrust belt.

Uplift and pene-planation led to the erosional truncation of the Carboniferous sequences and formation of the Base Permian Unconformity (BPU; Fig.3). Sedimentation was renewed during the Permian-Triassic when continental red beds onlapped and draped on to the BPU. The locus of basin subsidence lay to the west to create the EISB (Kirby *et al.* 2000); one of a series of major rifts that developed in response to east-west extension across the region. The development of the EISB was accommodated by large NNE-SSW striking normal faults that transect the Carboniferous structure (Fig.2). Some of the structures extend onshore to affect the Fylde area, with the local development of major normal faults to create local extensional depocentres, of which the Elswick Graben and Sollom sub-basin that cut through PEDL 165 represent prime examples (Fig.2; Clarke *et al.* 2018).

The basin continued to subside through the Mesozoic before being uplifted during the Cenozoic, which brought the Carboniferous, Permian and Triassic sediments back to outcrop (Holford *et al.* 2008). The Ribblesdale area is also transected by numerous, late, NW-SE striking extensional faults that include the Billsborrow and Grimsargh Faults (Fig.2). Since these structures offset the Permo-Triassic structures like the Woodsfold Fault (Fig.2), they clearly formed later and may form part of a suite of Cenozoic structures that developed in response to pervasive Atlantic plate-margin deformation (Underhill, 2009).

Stratigraphy

Litho- and Chrono-Stratigraphy

The Carboniferous stratigraphy of the Craven Basin is well displayed throughout the Ribblesdale Fold Belt and the Burnley Coalfield on its eastern margin. Distinct facies and thickness variations are seen between the basin depocentre and its margins during Dinantian

times (Fig. 3), something that reflects the bathymetry changes between upstanding blocks and intervening troughs resulting from (syn-rift) extension (Gawthorpe 1987).

Lower Dinantian (Tournaisian) and older rocks are absent from marginal blocks like the West Lancashire High, Askrigg Block and Lake District Massif, where deposition only began in the Visean (Arthurton *et al.* 1988). In these areas, condensed shallow to marginal marine platform carbonates (including those ascribed to the Great Scar Limestone Group) were established on highly deformed and weakly metamorphosed Upper Palaeozoic (Caledonian) roots before passing up into cyclical clastics ascribed to the Yoredale Group (Fig. 3).

In contrast, deposition in the basinal areas started earlier with deposition of red bed clastics like the Sedbergh Conglomerate Formation (Underhill *et al.* 1988) and sediments ascribed to the "Old Red Sandstone" in the Boulsworth borehole (Ramsbottom 1974). The earliest sediments known at surface in the Craven Basin are mudstones belong to the (Upper Courceyan (Ivorian)-Lower Chadian) Chatburn Limestone Formation (Fig. 3; Fewtrell & Smith 1980), which were also seen in the Swinden-1 borehole near Skipton (Charsley 1984).

The Chatburn Limestone Formation is overlain by the (Chadian-Asbian) Worston Shale (or Craven) Group, which includes Waulsortian reef knolls (Miller & Grayson 1972) and boulder beds (Dunnington 1945) belonging to the Clitheroe Limestone Formation in its lower section (Fewtrell & Smith 1980). The remainder of the succession consists of the (Late Chadian-Holkerian) Hodder Mudstone, (Holkerian) Hodderense Limestone and (late Holkerian-Asbian) Pendleside Limestone Formations (Earp *et al.* 1961; Fewtrell & Smith 1980; Aitkenhead *et al.* 1992).

The Bowland Shale Group (BSG) sits conformably upon the Worston Shale Group and consists of two component parts: the (Late Asbian-Brigantian) Lower Bowland Shale and (Pendelian) Upper Bowland Shale Formations, the contact between which is marked by the

Cravenoceras leion marine band (Aitkenhead *et al.* 1992) representing the boundary between the Dinantian and Silesian (Visean and Namurian). The upper boundary of the BSG is marked by the *Cravenoceras malhamense* marine band (Fig. 3). The BSG locally reaches thicknesses of over 1500m and is organic rich with Total Organic Carbon (TOC) values of up to 7% (Clarke et al., 2018). The unit is considered to be the main source rock for the oil and gas fields in the EISB (Lawrence *et al.* 1987; Armstrong *et al.* 1997) and East Midlands petroleum province (Fraser *et al.* 1990).

The Millstone Grit Group marks the onset of coarse clastic, southerly prograding deltaic sedimentation across Northern England (Collinson, 1969; Collinson, 1970; Steele, 1988; Hampson, 1997). The group can be subdivided into several component parts the most notable of which are the (Pendleian E1-E2a) Pendleton (or Pendle Grit) Formation, Warley Grit, Sabden Shales, Kinderscout Grit, Middle Grit and Rough Rock. Their recognition across the region suggests that basin subsidence was more uniform by Namurian times. Upper Carboniferous deposition is completed by the fluvial-deltaic sediments of the Coal Measures Group, the lower boundary for which is defined by the *Subcrenatum* marine band (Fig. 3).

A major unconformity separates folded and truncated Carboniferous sediments from a Permo-Triassic continental red bed succession, the base of which is marked by the Upper Permian (Rotliegend Group) Collyhurst Sandstone Formation and (Zechstein Group) Manchester Marl Formation (Fig. 3). Higher parts of the succession comprise the Sherwood Sandstone and Mercia Mudstone Group, which outcrop over western areas of Lancashire and extend offshore into the East Irish Sea. With the exception of the Preesall Halite that is developed in and around Fleetwood, none of the evaporites that characterise offshore parts of the EISB are developed in the Fylde area (Wilson 1990). Apart from a thin Quaternary cover, the Triassic represents the youngest solid-rock stratigraphy in the area because of the effects of Cenozoic uplift and erosion.

Seismic Stratigraphy

The variations in lithologies lead to changes in density and/or seismic velocities which in turn create acoustic impedance contrasts, which enable seismic interpretation. The most continuous stratigraphic surfaces that can be recognised and mapped are the BPU, which is marked by erosional truncation of Carboniferous sediments and structures, and by the onlap and drape by its Permo-Triassic cover. A marked regional seismic facies contrast marks the top of the Lower Bowland Shale Formation, which enables the component parts of the Bowland Shale Group to be mapped. Our interpretations have focused upon mapping these two prominent horizons and the base of the basinal Carboniferous, the results of which illustrate the main structural styles that characterise both the Ribblesdale Fold Belt and its Permo-Triassic (EISB) and younger tectonic overprint.

Data and Methods

Seismic Data

The Bowland-12 survey upon which this study is based was acquired in 2012 by CGG for Cuadrilla Resources. The 3D seismic volume covers a c.100km^2 area of the Fylde Peninsula (Fig. 4) and was released into the public domain in January 2018. We have gained access to the data as a result of public release through the UK Onshore Geophysical Library (UKOGL) and produced an interpretation thereof using Schlumberger Petrel software mounted on workstations housed at Heriot-Watt University. A processed zero-phase post-stack time-migrated volume was used for this study, where the data has been interpolated into a cube consisting of 427 inlines and 433 crosslines; with a horizontal spacing of 25m. Vertical

resolution at Bowland Shale level is approximately 40m based on an average frequency of 30Hz and velocity of 4800m/s.

The interpretation of the 3D volume has been combined with those derived from vintage regional 2D seismic data acquired in the 1980s and 90s as part of an earlier campaign of conventional hydrocarbon exploration including the UKOGL regional line published by Butler & Jamieson (2013). All of the seismic data are calibrated by 5 exploration wells (Table 1), leading to high confidence in the interpretations and mapping. All three shale-gas exploration wells drilled by Cuadrilla Resources, PNR-1, Preese Hall-1 and Grange Hill-1Z, have been integrated into the study to calibrate the seismic interpretation using their wireline logging suites, well reports and core studies. Electrical wireline logs and well reports for two legacy conventional British Gas wells (Thistleton-1 and Elswick-1) were also used. The shale-gas well data were provided by the British Geological Survey (BGS) and the legacy wells obtained via CGG's Data Management Service.

Well Ties and Seismic Interpretation

The wireline signature and seismic character at Grange Hill-1Z, Preese Hall-1 and PNR-1 wells are illustrated in Figure 5. Synthetic seismograms were created for each of the well locations and correlated with the adjacent seismic data. Use was then made of stratigraphic horizons marked by acoustic impedance reflections and their terminations to interpret the whole 3D data volume.

The most prominent horizons in the Permo-Triassic section belong to anhydrites of the Manchester Marl Formation and can be correlated between Preese Hall-1 and PNR-1 wells. As the underlying Collyhurst Sandstone Formation is poorly developed over much of the

study area, these provide a useful aid and are an effective proxy for mapping the Base-Permian Unconformity (BPU).

Reflectivity in the Carboniferous section also permits the main stratigraphic units to be recognised and key horizons to be mapped. The underlying Millstone Grit is characterised by a series of strong reflectors indicative of thick sand units interbedded with shales. Preese Hall-1 and Grange Hill-1Z penetrated a full Millstone Grit sequence, but it is absent in the PNR-1 well. The Upper Bowland Shale shows a contrasting seismic signature characterised by a lack of clear reflectivity. This formation consists mainly of silty shale interbedded with thin (5-10m thick), low impedance, shales and very thin (1-2m thick) high impedance, carbonates/siltstones. The individual thickness of these contrasting units however is below seismic resolution at this depth (c. 40m) and explains the lack of reflectivity response. Finally, the Lower Bowland Shale is characterised by the return of strong reflectors. These are produced by thicker (20-30m) low impedance shales interbedded with high impedance carbonates or sandstones (50-60m thick) which show a more distinctive seismic character visible at the base of the Grange Hill-1Z and Preese Hall-1 wells. While this unit can still be identified at the base of the PNR-1 well, reflection amplitude is notably lower than that observed in the other wells (Fig. 5).

Three NW-SE striking arbitrary dip sections (Figs.6-8), two (eastern and western) arbitrary strike lines (Fig. 9-10) and selective seismic timeslices (Figs.11-12) were initially used to tie the wells that lie within the seismic volume, constrain the horizon interpretation and identify the main faults. Good correlations were possible and no significant time shift was apparent at the three wells lending confidence to the wider interpretation seeded by these data. The time-depth relationships obtained from checkshot surveys in the Thistleton-1 and Elswick-1 wells

and vertical seismic profiles (VSPs) for Grange Hill-1Z, Preese Hall-1 and PNR-1 were also used in depth conversion to determine stratigraphic horizon depths and estimate bedding dips.

A number of key and consistent stratigraphic markers were apparent in the wells and these provided a basis upon which to extend interpretations across the whole survey. Although all the prominent stratigraphic horizons have been mapped, we use the two that are most relevant to illustrate the critical stratigraphic and structural geometries for shale gas exploration in the area in this paper, namely:

- The Base Permian (Variscan) Unconformity (BPU), which represents the boundary of high amplitude Permian Collyhurst Sandstones and lower amplitude, tilted and truncated Carboniferous sands and shales;

- The top of the Lower Bowland Shale, which represents the youngest hard calcareous sand unit within the shale.

The interpretation of the Bowland-12 survey using a combination of seismic sections and timeslices has enabled us to define the principal structural features that affect the Bowland Shale and offset the BPU. Horizon and fault mapping was carried out across the study area to identify the main structural elements and produce time structure maps. The maps were gridded using convergent interpolation and then displayed with overlays of the mapped fault planes (Figs. 13-14). In some parts of the survey, however, interpretation was limited by data quality and it has been necessary to infer fault traces or horizon picks honouring adjacent trends and regional knowledge.

The western strike line (Fig. 9) was deliberately selected in order to compare our interpretations with those described by Clarke *et al* (2018; their Fig.3b). However, we found

it impossible to replicate their line whilst honouring the check-shot calibrated stratigraphy in the Grange Hill-1Z well since the latter lay on the downthrown side (footwall) of a major, large-displacement fault, separating it from the corresponding upthrown (hangingwall) in which Preese Hall-1 well is situated. This fault is named here as the Summerer Fault after the farm and woods over which it is situated and may correspond to the PH-1 Fault first identified as present to the north of the Preese Hall-1 well by Oil & Gas Authority (2018). In order to duplicate Clarke *et al* (2018)'s line requires the Grange Hill-1Z well to be projected across the aforementioned fault and time shifted up by c.300ms, neither of which can be justified. As a consequence, we present a new interpretation for the three-well tied strike line that demonstrates the role of the Summerer Fault that is evident between the Grange Hill-1Z and Preese Hall-1 wells (Fig.9).

Permian-Triassic Structure

Permo-Triassic strata outcrop or lie beneath a thin Quaternary cover across the whole of the Bowland-12 3D seismic survey. In eastern areas of the survey, the disposition of the Permo-Triassic is affected by the occurrence of several NNE-SSW striking normal faults. The most significant structure is the WNW-dipping Woodsfold Fault, the surface trace of which lies outwith the 3D volume where it defines the NW limit of West Lancashire Coalfield (Kirby *et al.* 2000).

The Woodsfold Fault defines the eastern edge of a major graben, the Elswick Graben of Clarke *et al* (2018) and deeper parts of the fault are well imaged on the dip and strike lines (Figs.6-8 & 10) and time-slices (Figs.11-12), allowing the course of the structure to be mapped over the SE part of the survey (Figs.13-14). The western part of the graben is defined by three E-dipping (antithetic) faults (from east to west: the Elswick, Thistleton and Larbeck

faults (Aitkenhead *et al.* 1992) (Fig. 6). While the Elswick fault defines a terrace in the hangingwall to the large-displacement Thistleton Fault, the Larbeck Fault lies in the footwall to the Thistleton Fault and has a more modest offset. The faults are clearest observed on dip-sections in the north (Figs. 6-7), and the Thistleton and Elswick have been mapped throughout the seismic volume (Figs. 11 & 13). The southern part of the graben is separated by a large cross-fault which downthrows the Permo-Triassic and older sequences to the south (Fig. 10). This fault runs perpendicular to the Woodsfold and Thistleton Faults and is considered an example of a release fault (Destro, 1995) formed in response to differential displacement along the strike and in the hangingwall of the former. It is named herein as the Wesham Fault after village under which it lies.

The increase in thickness of the Manchester Marl Formation and presence of the Collyhurst Sandstone Formation in the graben (Figs.6-8 & 10) demonstrate that the fault systems were active during Permo-Triassic deposition. Folding of upper parts of the Triassic sequence to create the Kirkham Syncline and Elswick Anticline at outcrop (Wilson 1990; Aitkenhead *et al.* 1992) may be a consequence of compactional drape over a buried western terrace that forms the fault bound 3-way dip closure that hosts the Elswick gasfield itself (Fig. 13) or be a consequence of regional basin inversion.

One major effect of the Permo-Triassic extension is to add additional complexity to the Carboniferous section with NNE-SSW faults transecting the earlier NE-SW Variscan structures and a consequent lower level of confidence in horizon mapping beneath the BPU. In contrast to eastern parts of the survey, its occurrence in the Grange Hill-1Z and Preese Hall-1 wells and distinctive reflectivity demonstrate that the Permo-Triassic only forms a thin veneer to their Carboniferous subcrop in the west thus, allowing the Variscan structures that lie below to be mapped with confidence.

Although there is a complete absence of younger sediments in the area, porosity-depth plots, sonic velocity values and apatite fission track analysis all point to there having been a substantive (>1km) post-Triassic sedimentary cover in the area. Its removal is thought to have occurred in the Cenozoic in response to regional uplift and plate margin forces, the differential effects of which led to fault (re)activation. This mechanism may explain some of the normal fault offsets that affect the Permo-Triassic sequence in a similar way to that seen elsewhere in the UK (e.g. Argent *et al.* 2002; Guariguata-Rojas & Underhill 2017).

Carboniferous Structure

Mapping of the Lower Bowland Shale has highlighted the severity of deformation in the area, which manifests itself as a series of high-angle reverse faults (that result from the contractual reactivation of normal fault precursors (tectonic inversion structures)) and by the folding and erosion of Carboniferous sequences. These features are best demonstrated through the use of three dip-lines (Figs. 6-8), two strike lines (Figs. 9-10) and a timeslice extracted at 1200ms (Fig. 12).

A short dip-line in the NW of the survey tieing the Grange Hill-1Z and Elswick-1 wells with the site of the proposed Roseacre Wood pad illustrates the presence of large reverse faults affecting the Carboniferous sequences (Fig. 6). To the west of the Grange Hill-1Z well, a SE-dipping reverse fault with a throw of c. 300ms (c. 1km) is present separating the block in which the well targeted from an un-drilled deeper block at 1800ms (c. 3880m). This fault is considered the northwards continuation of the Haves Ho Fault identified in the operator's hydraulic fracture plans for PNR-1Z and PNR-2 wells (Cuadrilla Resources, 2018a, b). To the east of the well, another SE-dipping reverse fault with a throw of c. 300ms (c. 1km) separates this block from another characterised by steeply dipping continuous reflectors. This

fault is the aforementioned Summerer Fault. Further south-east, the Millstone Grit is truncated beneath the BPU in the footwall of another SE-dipping reverse fault (considered synonymous with the Moor Hey Fault of Cuadrilla Resources (2018 a, b)), resulting in the Upper Bowland Shale being brought directly beneath the unconformity. Within the hangingwall of the Thistleton Fault and within the Elswick Graben, the Upper and Lower Bowland Shale are buried beneath a thicker Permo-Triassic section. Elswick-1 was completed in a Carboniferous sequence, and the corresponding stratigraphic top lies directly beneath a strong reflector interpreted as the BPU.

A long dip-line tieing the Preese Hall-1 and Thistleton-1 wells further illustrates the structural features (Fig. 7). The Haves Ho and Summerer Faults appear to begin to converge and the block in which Grange Hill-1Z was drilled narrows. The seismic facies of the Lower Bowland Shale between the two tied wells is that of continuous but steeply-dipping (c. 30°) reflectors. Within the Elswick Graben, the Lower Bowland Shale is present at a shallower depth than observed in Fig. 6 and a small west-dipping reverse fault is identified.

A dip-line that ties the PNR wells illustrates a contrasting picture (Fig. 8). The Haves Ho and Summerer Faults are absent on this line. The Lower Bowland Shale is present at c. 1200ms (c. 2270m) depth and is characterised as a series of gently undulating low amplitude reflectors. The Moor Hey Fault is present east of the well although reflectivity is very limited in the hangingwall. Within the hangingwall of the Thistleton Fault a thick Triassic sequence is present, burying the Carboniferous to c. 1200ms (c. 2270m). The Lower Bowland Shale is interpreted as absent in this area.

Use of a composite section along the strike of the major structures (Fig. 9) and predominantly within the block between the Preese Hall-1 and Thistleton-1 wells illustrates a more continuous section but not one without structure complexity. The Summerer Fault is present

between the Grange Hill-1Z and Preese Hall-1 wells. To the south, the Carboniferous sequences are brought up to beneath the BPU with the Millstone Grit truncating beneath the unconformity prior north of PNR wells. These wells found Upper Bowland Shale to lie directly beneath the unconformity.

The features identified in these cross-sections were interpreted throughout the entire 3D volume and have allowed us to map the Lower Bowland Shale surface and associated fault planes. This has concluded that the Bowland Shale is dissected into discrete fault-bound compartments, four of which can be mapped within the footwall of the Thistleton Fault (Fig. 12):

- *Poulton Block*

Positioned in the far NW of the survey region, the Poulton block (named after the business park situated above it) contains the Lower Bowland Shale buried to a depth of around 1800ms TWT (c. 3880m) (Figs 6-7, 12 & 14). The structural compartment ranges in width from between 800m and 2.5km between the edge of the survey and the Haves Ho Fault which defines the block to the SE. The Lower Bowland Shale forms a small syncline in the block which dips steeply (c. 50°) to the SE and terminates against the Haves Ho Fault. This block is un-drilled to-date and has been mapped based purely on seismic character.

- *Singleton Block*

Named after the village beneath which the fault-bound compartment lies, the Singleton Block forms a narrow compartment separated from the Poulton Block by the Haves Ho Fault (Figs. 6-7, 9, 12, & 14). The block is 1.5km wide in the north and narrows to the south-west. It is

defined in the east by the Summerer Fault. The Grange Hill-1Z well drilled in 2010 targeted the Bowland Shale within this specific fault block.

- *Weeton Block*

The largest fault block is separated from the Singleton block by the Summerer Fault. Its easternmost limit is defined the Moor Hey Fault. We have termed this fault-bound compartment the Weeton Block after the most significant village lying above the feature (Figs. 6-7, 9, 12 & 14). It is synonymous with what Cuadrilla have termed the "Thistleton fairway". The throw of the Moor Hey Fault is estimated at c. 300m but this is uncertain due to lack of clear reflectivity in the area. The width of this block is the largest of those we can identify and varies from between 1.5 and 3.2km. The compartment hosts the Thistleton-1, Preese Hall-1 and PNR-1, PNR-1Z and PNR-2 wells (Fig.14). The block can be further subdivided into two contrasting portions. Towards the south and west, there is little deformation and beds are generally sub-horizontal (Fig.9; PNR well location). Towards the north and east, there is evidence of stronger deformation with steeply dipping beds east of the Preese Hall-1 well (c. 30°) and further reverse faulting and folding present up to the Moor Hey fault (Figs.6-7). The Millstone Grit is folded to the south and east and truncated beneath the Base-Permian Unconformity in the footwall of the Moor Hey Fault, positioning the Upper Bowland Shale directly beneath the Permian sequences. Reflector strength begins to diminish in the east of this block making for a more challenging interpretation and some uncertainty to the mapping in that sub-area.

- *Greenhalgh Block*

The final fault-bound compartment to be identified in the footwall of the Thistleton Fault is the Greenhalgh Block. The structural domain is defined in the west by the Moor Hey Fault and to the east by the Thistleton Fault. We have named it after the village of Greenhalgh that lies directly above the feature. The compartment forms a narrow block (max width of 1.5km), where reflectivity is very limited, but the Upper Bowland Shale is interpreted as present at c. 600ms (c. 950m) directly beneath the BPU.

Other fault-bound compartments can be identified in the tract beneath the Elswick Graben in the SE part of the survey. However, the inherent structural complexity imposed by the subsequent Permo-Triassic extensional structures and their offsets has caused the Carboniferous sequences to be dissected and mapping of the compartments containing the Bowland Shale is all the more challenging. As a consequence, we have not sought to define or name individual compartments in this area in the way that has proved possible to do in the area affected to the north-west, where the effects of Permo-Triassic extension are absent.

We interpret the compartments defined by our mapping as the buried extension to the Ribblesdale Fold Belt since the structural signature observed is entirely consistent with the steep reverse faults and NE-SW striking asymmetric anticlines that characterise areas to the northeast. The results of the seismic interpretation allow us to reconstruct the development and evolution of the area (Fig.15). While the structural geometries for the Variscan reverse faults are consistent with dip-slip contractional reactivation of normal faults (structural inversion) proposed by Gawthorpe (1987). However, we are mindful that our observations are at a seismic scale and so a component of strike- or oblique-slip (transpression) as proposed by Arthurton (1984), may also play a role.

Implications for Shale Exploration

Reserve Estimates and Optimal Drilling Locations

An understanding of the subsurface structure is vital in any shale resource assessment and when seeking to evaluate the risk of intersecting critically stressed faults, upon which seismicity might be induced. Due to shale's low permeability, it is necessary to hydraulically fracture the rock at multiple stages along a horizontal well in order to initiate the flow of hydrocarbons. As such, long-reaching lateral wells are required in order to maximize contact with productive shale horizons and ensure the viability of the play. As an example, typical lateral sections within the Lower Carboniferous Barnett Shale play of the Appalachians in the USA usually have lengths of between 600m and 1800m (Yuan *et al.* 2017). Furthermore, given the rapid decline in flow, it is necessary to drill wells at a close spacing during intense drilling programmes in order to produce hydrocarbons at commercial rates (Baranzelli *et al.* 2015; Clancy *et al.* 2018). Pad-based drilling allows this to be achieved efficiently whereby multiple wells are drilled in varying directions out from a single surface location.

As our mapping has shown, the Bowland Shale is folded and transected by several large displacement faults, the combined effects of which lead to irregular bedding dips and create fault-bound compartments, the maximum width of which (3.2 km) occurs in the Weeton Block. Not only does this restrict the connected shale resource in the Fylde area, it also provides a constraint upon the drilling of long laterals in the optimal direction to maximise production. Similar structural challenges have been recognised in other areas of the UK, such as the Midland Valley of Scotland (Underhill et al., 2008), where shale gas extraction is likely to be equally challenged (Underhill, 2019).

The productive shale plays in North America and Argentina are largely characterised by shallow dips, a lack of folding and absence of large faults, leading to lateral continuity of target horizons. In such relatively undeformed areas, wells are preferentially drilled such that fractures will propagate in the direction of the greatest principal stress (usually the maximum horizontal stress (SHMAX) direction in deep reservoirs). Therefore, horizontal sections are typically drilled to align with the minimum horizontal stress orientation. There is limited borehole information available to determine SHMAX orientation. Kingdon *et al* (2016) report a mean SHMAX orientation of 154.5° from the Sellafield borehole whereas Clarke *et al* (2018) report mean SHMAX orientations of 173°, values that are consistent with regional data (Heidbach *et al.* 2016).

Based on the regional stress data, it would be necessary to drill horizontal wellbores at an azimuth of between 60-80° (WSW-ENE) in order to most effectively fracture the formation (Fig.16 (c) and (d)). However, as our mapping in the area has shown, the structural grain imposed by Upper Paleozoic (Carboniferous, Variscan and Permian) and younger activity comprises two main, WSW-ENE and SSW-NNE fault networks which both complicate the subsurface structure and place a major constraint on exploration. Using this wellbore orientation, even in the widest (Weeton) block, where the effects of the Permo-Triassic structure is absent, the spacing of the Variscan block-bounding steep, reverse faults restrict the maximum length to 4.2km (Fig. 16(b)).

A variation in bedding dip can also be observed within each major fault compartment, usually associated with smaller-scale faulting which will also provide a constraint upon where low-angle lateral wells can be drilled. In order to investigate this, a bedding dip angle map was calculated using a depth-converted Lower Bowland Shale surface and the region was classified based on dip angle cut-offs and reflector continuity (Fig. 16 (a) and (b)). This

approach allows us to define four main common risk segments from which it is apparent that PNR, Grange Hill-1Z and the previously-proposed site at Roseacre Wood lie in the most prospective areas characterised by bedding dips <30° and where there is good reflector continuity (Fig.16b). While a 4.2km lateral could potentially be achieved within the Weeton Block at a drilling azimuth of 60-80°, the occurrence of high bedding dips, particularly in areas situated to the east of Preese Hall-1 adversely impacts prospectivity. The most prospective region then limited to an area around the PNR site with a maximum width of 1.9km (Fig. 16(b)).

One additional, significant consequence is that the optimal well pad locations lie along the eastern margin of a compartment since that potentially allows the maximum lateral length of a wellbore to be drilled in continuous and largely undisturbed horizons outwith and away from zones of step dip (Fig.16b). It is apparent that the Grange Hill-1Z well lies in a narrow compartment, Preese Hall-1 is situated on the western side of another and only PNR is positioned to the east of a compartment with the possibility to drill a longer lateral in the desired direction through gently dipping shale target horizons (Fig.16b).

Avoiding major structures could pose a significant challenge if drilling along the azimuth of WSW-ENE. To counteract the effect of the spatial limits imposed by the fault-bound blocks and achieve maximum (commercial) flow rates might necessitate the hydraulic fracture of numerous, vertically stacked, multi-lateral wells that target specific and numerous benches within the Bowland Shale. Naturally, adopting such an approach also pre-supposes several intervals with high Total Organic Carbon (TOC), suitable geomechanical properties (Anderson *et al.* 2019) and sufficient gas yields to be present; the latter of which has been recently been challenged by Whitelaw et al. (2019).

Induced Seismicity on Seismically Resolvable Faults

Fault reactivation and induced seismicity are well documented during hydraulic fracturing operations. They are triggered by stress changes in the rock mass following injection, or by pore pressure changes along a permeable fault zone (Bao & Eaton 2016). Attempts have been made to quantify the distance at which a fault may be at risk of reactivation during hydraulic fracturing operations (Westwood *et al.* 2017) where the authors modelled 'respect distances' of between 63m and 433m. However, this clearly limited to those faults which are seismically resolvable and critically stressed. Our mapping has demonstrated the Lower Carboniferous to be heavily structured by seismically resolvable faults which would limit the areas in which hydraulic fracturing could occur using even the maximum respect distance proposed by Westwood *et al* (2017).

In 2011, prior to the acquisition of the Bowland-12 dataset, a hydraulic fracturing program consisting of five fracture treatments across a 1000m section of the Bowland Shale was carried out at Preese Hall-1 (Clarke *et al.* 2014). A total of 50 seismic events were recorded during and after operations; the largest two of which (M_L=1.5 and M_L=2.3) occurred 10 hours after shut-in of stages 2 and 4 respectively (De Pater & Baisch 2011; Green *et al.* 2012). These events led to a review of the government regulations on induced seismicity around hydraulic fracturing operations and ultimately the development of a "Traffic Light System". This scheme still remains in-place and requires the cessation of operations, and the re-adjustment of fluid pressures/injection volumes if events of 0.5M_L or larger occur (Green *et al.* 2012).

De Pater & Baisch (2011) reviewed a number of geomechanical and microseismic studies focusing on the Preese Hall-1 well and concluded that reactivation of a critically stressed pre-existing fault was the likely mechanism for the explaining patterns of induced seismicity.

Following acquisition of the 3D seismic survey in 2012, Clarke *et al* (2014) used a microseismic event recorded during the flowback phase with better spatial constraint to locate a previously un-mapped fault directly to the east (Fig. 7) of the well. While their analysis is not disputed, the Summerer reverse fault mapped herein is interpreted to lie directly north and west of the well and we speculate as to whether it may also have played a role in the induced seismicity recorded.

The Role of Sub-Seismic Faulting

The experience at Preese Hall-1 stresses the importance of the identification of faults using high-quality 3D seismic data prior to any hydraulic fracturing operations. However, the limited vertical resolution of modern-day seismic data places a minimum constraint on the size of fault and associated displacement that an interpreter can confidently identify and map. As mentioned previously, the vertical resolution at Bowland level is approximately 40m but it seems likely that in such a structurally complex area there are further faults with displacements below this cut-off that cannot be observed using this dataset. The nearby East Pennines Coalfield provides an analogue where fault patterns have been extensively studied within the Westphalian Coal Measures (Walsh & Watterson 1988; Watterson *et al.* 1996; Bailey *et al.* 2005) and those authors found a dense fault network of 7.58 faults per km^2 (Bailey *et al.* 2005; Westwood *et al.* 2017) with throws as little as 0.91m (Bailey *et al.* 2005).

In 2018, hydraulic fracturing operations were undertaken at the PNR-1Z lateral well. Fifteen hydraulic fracture tests were made (of a planned 41) and resulted in the recording of 38,383 microseismic events of which nine were reported to the Regulator under the aforementioned traffic light system. This led to four suspensions in drilling operations. Six of these large

events occurred during pumping and three (including the largest M_L=1.5) were trailing events (Cuadrilla Resources 2019).

Clarke *et al* (2019) produced maps (their Fig. 5) showing the unusual pattern of microseismic events around the PNR-1Z well notably the northwards propagation away from each stage and an overall SW-NE trend. Their analysis of the microseismic focal mechanisms, events with ML>0 and cumulative seismic moment led them to identify a sub-seismic plane striking at 237° and dipping at 70°, which was argued to be the cause of microseismic pattern. Such structure would be impossible to identify within the limits of modern seismic reflection seismic data but a case can be made for real-time identification of these structures if operations can be adjusted accordingly.

Taken together, our results underline how important it is to characterise and understand the subsurface geology and regional stress field prior to the drilling of, and hydraulic fracturing along, long horizontal wells. The acquisition and accurate interpretation of high-quality 3D seismic datasets is crucial when seeking to identify and map all faults including those that may be critically stressed prior to fluid injection. The induced seismicity at the Preese Hall-1 well supports this. However, exploration in such a structured area also highlights risks that cannot be mitigated through analyses of seismic data alone. The experience at PNR-1Z confirms this and poses serious questions as to whether sub-seismic faulting is pervasive, induced seismicity is to be expected and how it should be planned for prior to hydraulic fracturing operations. Further induced seismicity has subsequently been recorded with magnitudes up to 2.9M_L at the PNR-2 well (Oil & Gas Authority 2019).

Conclusions

Integration of regional geology, the analysis of exploration wells and the interpretation of a newly released 3D seismic volume highlight the structural complexity of the Craven Basin in the Fylde area of NW Lancashire and its impact for shale gas exploration. The results demonstrate that Lower Carboniferous (Dinantian- Early Namurian) Bowland Shale targets are affected by a suite of folds and faults resulting from syn-sedimentary extension, Variscan contraction that led to large offset reverse faulting and basin inversion, renewed extension in the Permo-Triassic and renewed movement during subsequent Cenozoic uplift and exhumation. Structuration is more intense beneath the BPU and is consistent with it being part of the SW-extension to the Ribblesdale Fold Belt that is exposed along strike. Variscan folds and steep reverse faults together with other structures resulting from subsequent Permo-Triassic extension and Cenozoic events, define elongate fault-bound compartments containing steep and variable bedding dips. The occurrence, size and dimensions of the compartments places limits on shale resources, the optimal location of well sites and on horizontal well bore lengths. The accurate mapping of faults prior to the drilling and hydraulic fracturing of wells may also help reduce the risk of fault reactivation and induced seismicity. However, in such a structurally complex area, sub-seismic faults should also be anticipated, and plans drawn up to mitigate for their reactivation. Our structural interpretations suggest that the Bowland Shale gas play remains highly challenged with significant uncertainty in its resource estimates, the planning of well site locations, horizontal wellbore pathways and risk of induced seismicity on faults that are seismically resolvable and those that are sub-seismic scale.

Acknowledgements

Jingsheng Ma, Xiaoyang Wu, Dorrik Stow and David Griffiths are all thanked for their input and discussion. Malcolm Butler, Mark Alldred and Neil Anderson are acknowledged for providing access to the data via the UK Onshore Geophysical Library (UKOGL). The British Geological Survey (BGS) and Compagnie Générale de Géophysique (CGG) are thanked for providing access to well data, and Schlumberger are thanked for the provision of Techlog and Petrel software under academic license to Heriot-Watt University. We acknowledge use of the Ogilvie-Gordon 3D Audio-Visualisation Centre (OGAVC) in Heriot-Watt Wing of the Lyell Centre as an aid in guiding and honing our subsurface interpretations of the structure contained within the Bowland-12 seismic survey. We appreciate Stavros Vrachliotis' assistance when using the facility. Jon Walsh and Richard Wrigley are thanked for their constructive and helpful reviews and Graham Yielding is acknowledged for his editorial support.

Funding

Iain Anderson acknowledges the support of a James Watt Scholarship from Heriot-Watt University (HWU) and the receipt of a British University Funding Initiative (BUFI) studentship award (grant no. GA/16S/024) from the British Geological Survey (BGS), which provides the funding for the PhD project upon which this work is based. The PhD. forms part of the Natural Environment Research Council (NERC) Centre for Doctoral Training (CDT) in Oil and Gas (grant no. NE/M00578X/1), a UK-wide, flagship research and training programme partnership of 17 universities and 2 NERC research centres led and managed by HWU. The Ph.D. research forms part of the CDT's Unconventional Oil & Gas Resources theme.

References

Aitkenhead, N., Bridge, D. McC., Riley, N.J. & Kimbell, S.F. 1992. *Geology of the Country around Garstang. Memoir for the 1:50 000 Geological Sheet 67*. HMSO, London, British Geological Survey, HMSO, London.

Anderson, I., Ma, J., Wu, X., Stow, D. & Underhill, J.R. 2019. Assessing The Stratigraphic Variations In Geomechanical Properties Of The United Kingdom Bowland Shale Using Wireline And Seismic Data: How Could These Guide The Placement Of Lateral Wells? *In*: *URTEC-2019-257-MS* – SPE/AAPG/SEG Unconventional Resources Technology Conference. URTEC, Unconventional Resources Technology Conference, 14. https://doi.org/10.105530/urtec-2019-257.

Andrews, I.J. 2013. *The Carboniferous Bowland Shale Gas Study: Geology and Resource Estimation*. British Geological Survey for the Department of Energy and Climate Change (DECC). Andrews, I.J. 2014. *The Jurassic Shales of the Weald Basin: Geology and Shale Oil and Shale Gas Resource Estimation*. British Geological Survey for the Department of Energy and Climate Change (DECC).

Argent, J., Stewart, S.A., Green, P. & Underhill, J.R. 2002. Heterogeneous exhumation in the Inner Moray Firth, UK North Sea: constraints from new apatite fission track analysis and seismic data. Journal of the Geological Society, **159**, 715-729. https://doi.org/10.1144/0016-764901-141.

Armstrong, J.P., Smith, J., D'Elia, V.A.A. & Trueblood, S.P. 1997. The occurrence and correlation of oils and Namurian source rocks in the Liverpool Bay-North Wales area. *Geological Society, London, Special Publications*, **124**, 195–211. https://doi.org/10.1144/GSL.SP.1997.124.01.12.

Arthurton, R.S. 1984. The Ribblesdale fold belt, NW England—a Dinantian-early Namurian dextral shear zone. *Geological Society, London, Special Publications*, **14**, 131-137. https://doi.org/10.1144/GSL.SP.1984.014.01.13.

Arthurton, R.S., Johnson, E.W. & Mundy, D.J.C. 1988. *Geology of the Country around Settle*. Memoir of the British Geological Survey, Sheet 60 (England and Wales). HMSO, London.

Bailey, W.R., Walsh, J.J. & Manzocchi, T. 2005. Fault populations, strain distribution and basement fault reactivation in the East Pennines Coalfield, UK. *Journal of Structural Geology*, **27**, 913–928. https://doi.org/10.1016/j.jsg.2004.10.014.

Bao, X. & Eaton, D.W. 2016. Fault activation by hydraulic fracturing in western Canada. *Science*, **354**, 1406–1409. https://doi.org/10.1126/science.aag2583.

Baranzelli, C., Vandecasteele, I., Ribeiro Barranco, R., Mari i Rivero, I., Pelletier, N., Batelaan, O. & Lavalle, C. 2015. Scenarios for shale gas development and their related land use impacts in the Baltic Basin, Northern Poland. *Energy Policy*, **84**, 80–95. https://doi.org/10.1016/j.enpol.2015.04.032.

Brandon, A., Aitkenhead, N., Crofts, R.G., Ellison, R.A., Evans, D.J. & Riley, N.J. 1998. *Geology of the Country around Lancaster. Memoir for 1:50 000 geological sheet 59*. British Geological Survey. HMSO, London.

Butler M. & Jamieson R. 2013. Preliminary Interpretation of Six Regional Seismic Profiles Across Onshore Basins of England. UK Onshore Geophysical Library, digital publication.

Chadwick, R.A. & Evans, D.J. 2005. *A Seismic Atlas of Southern Britain : Images of Subsurface Structure*. Nottingham, UK, British Geological Survey.

Charsley, T.J. 1984. *Early Carboniferous Rocks of the Swinden No. 1 Borehole, West of Skipton*. **16/1**, British Geological Survey Report.

Clancy, S.A., Worrall, F., Davies, R.J. & Gluyas, J.G. 2018. An assessment of the footprint and carrying capacity of oil and gas well sites: The implications for limiting hydrocarbon reserves. *Science of the Total Environment*, **618**, 586–594. https://doi.org/10.1016/j.scitotenv.2017.02.160.

Clarke, H., Eisner, L., Styles, P. & Turner, P. 2014. Felt seismicity associated with shale gas hydraulic fracturing: The first documented example in Europe: Hydraulic fracturing, induced seismicity. *Geophysical Research Letters*, **41**, 8308–8314. https://doi.org/10.1002/2014GL062047.

Clarke, H., Turner, P., Bustin, R.M., Riley, N. & Besly, B. 2018. Shale gas resources of the Bowland Basin, NW England: a holistic study. *Petroleum Geoscience*, 24, 287-322. https://doi.org/10.1144/petgeo2017-066.

Clarke, H., Verdon, J.P., Kettlety, T., Baird, A.F. & Kendall, J. 2019. Real-Time Imaging, Forecasting, and Management of Human-Induced Seismicity at Preston New Road, Lancashire, England. *Seismological Research Letters*, 90, 1902-1915. https://doi.org/10.1785/0220190110.

Collinson J.D. 1969. The sedimentology of the Grindslow Shales and Kinderscout Grit, a deltaic complex in the Namurian of northern England. Journal of Sedimentary Petrology, **39**, 194-221. https://doi.org/10.1306/74D71C17-2B21-11D7-8648000102C1865D

Collinson J.D. 1970. Deep channels, massive beds and turbidity current genesis in the Central Pennine Basin. Proceedings of the Yorkshire Geological Society, **37**, 495-520. https://doi.org/10.1144/pygs.37.4.495

Corfield, S.M., Gawthorpe, R.L., Gage, M., Fraser, A.J. & Besly, B.M. 1996. Inversion tectonics of the Variscan foreland of the British Isles. *Journal of the Geological Society*, **153**, 17–32. https://doi.org/10.1144/gsjgs.153.1.0017.

Cuadrilla Resources. 2018a. Hydraulic Fracture Plan PNR 1/1Z. https://consult.environment-agency.gov.uk/onshore-oil-and-gas/information-on-cuadrillas-preston-new-road-site/supporting_documents/PNR1z%20Hydraulic%20Fracture%20Plan.pdf.

Cuadrilla Resources. 2018b. Hydraulic Fracture Plan PNR 2. https://consult.environment-agency.gov.uk/onshore-oil-and-gas/information-on-cuadrillas-preston-new-road-site/user_uploads/pnr-2-hfp-v3.0.pdf

Cuadrilla Resources. 2019. Preston New Road-1z: LJ/06-09(z) HFP Report. https://www.ogauthority.co.uk/media/5845/pnr-1z-hfp-report.pdf.

De Pater, C.J. & Baisch, S. 2011. Geomechanical study of Bowland Shale seismicity. *Synthesis report*, **57**.

Destro, N. 1995. Release fault: A variety of cross fault in linked extensional fault systems, in the Sergipe-Alagoas Basin, NE Brazil. *Journal of Structural Geology,* **17**, 615-629. https://doi.org/10.1016/0191-8141(94)00088-H.

Dunnington, H.V. 1945. Contemporaneous slumping in the Embsay Limestone series of the Skipton Anticline. *Proceedings of the Yorkshire Geological Society*, **25**, 239–247. https://doi.org/10.1144/pygs.25.4.239.

Earp, J.R., Magraw, D., et al. 1961. *Geology of the Country around Clitheroe and Nelson : One Inch Geological Sheet 68, New Series*. Geological Survey of Great Britain. England and Wales.

Fewtrell, M.D. & Smith, D.G. 1980. Revision of the Dinantian stratigraphy of the Craven Basin, N England. *Geological Magazine*, **117**, 37-49. https://doi.org/10.1017/S0016756800033082.

Fraser, A.J. & Gawthorpe, R.L. 1990. Tectono-stratigraphic development and hydrocarbon habitat of the Carboniferous in northern England. *In*: Hardman, R.F.P. & Brooks, J. (Eds.): *Tectonic Events Responsible for Britain's Oil and Gas Reserves*. *Geological Society, London, Special Publications*, 55, 49–86. https://doi.org/10.1144/GSL.SP.1990.055.01.03.

Fraser, A.J. & Gawthorpe, R.L. 2003. *An Atlas of Carboniferous Basin Evolution in Northern England*. *Geological Society, London, Memoirs*, 28. https://doi.org/10.1144/GSL.MEM.2003.028.

Fraser, A.J., Nash, D.F., Steele, R.P. & Ebdon, C.C. 1990. A regional assessment of the intra-Carboniferous play of Northern England. In: J. Brooks, J. (Ed.) *Classic Petroleum Provinces. Geological Society, London, Special Publications*, **50**, 417–440. https://doi.org/10.1144/GSL.SP.1990.050.01.26.

Gawthorpe, R.L. 1987. Tectono-sedimentary evolution of the Bowland Basin, N England, during the Dinantian. *Journal of the Geological Society*, **144**, 59–71. https://doi.org/10.1144/gsjgs.144.1.0059.

Glennie, K. & Underhill, J.R. 1998. Origin, Development and Evolution of Structural Styles. *In*: Glennie, K. (ed.) *Petroleum Geology of the North Sea*. https://doi.org/10.1002/9781444313413.

Green, C., Styles, P. & Baptie, B. 2012. *Preese Hall Shale Gas Fracturing: Review & Recommendations for Induced Seismic Mitigation*. London, England, Department of Energy & Climate Change.

Guariguata-Rojas, G.J. & Underhill, J.R. 2017. Implications of Early Cenozoic uplift and fault reactivation for carbon storage in the Moray Firth Basin. *Interpretation*, **5**, SS1–SS21. https://doi.org/10.1190/INT-2017-0009.1/

Hampson, G.J. 1997. A Sequence Stratigraphic model for deposition of the Lower Kinderscout Delta; an Upper Carboniferous turbidite-fronted delta. Proceedings of the Yorkshire Geological Society, **51**, 273-296. https://doi.org/10.1144/pygs.51.4.273

Harvey, A.L., Andrews, I.J. & Monaghan, A.A. 2018. Shale prospectivity onshore Britain. In: Bowman, M. & Levell, B. (eds) 2018. Petroleum Geology of NW Europe: 50 Years of Learning – Proceedings of the 8th Petroleum Geology Conference. *Geological Society, London, Petroleum Geology Conference series*, **8**, 571–584. https://doi.org/10.1144/PGC8.15.

Heidbach, O., Rajabi, M., Reiter, K., Ziegler, M. & WSM Team (2016). 2016. World Stress Map Database Release 2016. V. 1.1. *GFZ Data Services*. https://doi.org/10.5880/WSM.2016.001.

Hennissen, J.A.I., Hough, E., Vane, C.H., Leng, M.J., Kemp, S.J. & Stephenson, M.H. 2017. The prospectivity of a potential shale gas play: An example from the southern Pennine Basin (central England, UK). *Marine and Petroleum Geology*, **86**, 1047–1066. https://doi.org/10.1016/j.marpetgeo.2017.06.033.

Holford, S.P., Green, P.F., Turner, J.P., Williams, G.A., Hillis, R.R., Tappin, D.R. & Duddy, I.R. 2008. Evidence for kilometre-scale Neogene exhumation driven by compressional deformation in the Irish Sea basin system. *Geological Society, London, Special Publications*, **306**, 91-119. https://doi.org/10.1144/SP306.4.

Hughes, F., Harrison, D., et al. 2018. The unconventional Carboniferous reservoirs of the Greater Kirby Misperton gas field and their potential: North Yorkshire's sleeping giant. *Geological Society, London, Petroleum Geology Conference series*, **8**, 611–625. https://doi.org/10.1144/PGC8.5.

Kingdon, A., Fellgett, M.W. & Williams, J.D.O. 2016. Use of borehole imaging to improve understanding of the in-situ stress orientation of Central and Northern England and its implications for unconventional hydrocarbon resources. *Marine and Petroleum Geology*, **73**, 1–20. https://doi.org/10.1016/j.marpetgeo.2016.02.012.

Kirby, G.A., Baily, H.E., et al. 2000. *Structure and Evolution of the Craven Basin and Adjacent Areas*. British Geological Survey, Subsurface Geology Memoirs. HMSO, London.

Könitzer, S.F., Stephenson, M.H., Davies, S.J., Vane, C.H. & Leng, M.J. 2016. Significance of sedimentary organic matter input for shale gas generation potential of Mississippian Mudstones, Widmerpool Gulf, UK. Review of Palaeobotany and Palynology, 224, 146-168. https://doi.org/10.1016/j.revpalbo.2015.10.003

Lawrence, S.R., Coster, P.W. & Ireland, R.J. 1987. Structural development and petroleum potential of the northern flanks of the Bowland Basin (Carboniferous) North-west

England. *In*: Brooks, J. & Glennie, K. (Eds.): *Petroleum Geology of North West Europe*. 225–233.

Leeder, M.R. 1982. Upper Palaeozoic basins of the British Isles—Caledonide inheritance versus Hercynian plate margin processes. *Journal of the Geological Society*, **139**, 479–491. https://doi.org/10.1144/gsjgs.139.4.0479.

Miller, J. & Grayson, R.F. 1972. Origin and structure of the lower Visean "reef" limestones near Clitheroe, Lancashire. *Proceedings of the Yorkshire Geological Society*, **38**, 607–638. https://doi.org/10.1144/pygs.38.4.607.

Monaghan, A.A. 2014. *The Carboniferous Shales of the Midland Valley of Scotland: Geology and Resource Estimation*. British Geological Survey for the Department of Energy and Climate Change (DECC).

Moseley, F. 1962. The structure of the south-western part of the Sykes Anticline, Bowland, West Yorkshire. *Proceedings of the Yorkshire Geological Society*, **33**, 287-314. https://doi.org/10.1144/pygs.33.3.287.

Newport, L.P., Aplin, A.C., Gluyas, J.G., Greenwell, H.C. & Gröcke, D.R. 2016. Geochemical and lithological controls on a potential shale reservoir: Carboniferous Holywell Shale, Wales. Marine and Petroleum Geology, 71, 198-210. https://doi.org/10.1016/j.marpetgeo.2015.11.026.

Newport, S.M., Jerrett, R.M., Taylor, K.G., Hough, E. & Worden, R.H. 2018. Sedimentology and microfacies of a mud-rich slope succession: in the Carboniferous Bowland Basin, NW England (UK). Journal of the Geological Society, 175, 247–262. https://doi.org/10.1144/jgs2017-036.

Oil & Gas Authority. 2018. Summary note for OGA interpretation of BOWLAND-12 3D seismic integrating drilling results from PNR1, PNR1Z and PNR2 wells. https://www.whatdotheyknow.com/request/530205/response/1287502/attach/3/Summary%20note%20for%20OGA%20interpretation%20of%203D%20seismic%20data%20integrating%20drilling%20results%20from%20PNR%20wells%20Redacted.pdf

Oil & Gas Authority. 2019. Hydraulic fracturing at Preston New Road suspended. *Hydraulic fracturing at Preston New Road suspended.* https://www.ogauthority.co.uk/news-publications/news/2019/hydraulic-fracturing-at-preston-new-road-suspended.

Pharaoh, T., Haslam, R., Hough, E., Kirk, K., Leslie, G., Schofield, D. & Heafford, A. 2019. The Môn-Deemster-Ribblesdale Fold-Thrust Belt, Central UK: a concealed Variscan inversion belt located on weak Caledonian crust. In: Hammerstein, J.A., Di Cuia, R., Cottam, M.A., Zamora, G. & Butler, R.W.H. (Eds.): Fold and Thrust Belts: Structural Style, Evolution and Exploration. *Geological Society, London, Special Publications*, 490-in press; https://doi.org/10.1144/SP490-2018-109.

Ramsbottom, W.H.C. 1974. Dinantian. *In*: *The Geology and Mineral Resources of Yorkshire*. Occasional Publication of the Yorkshire Geological Society, 47–73.

Roche, I. 2012. Lessons from History - Unlocking a new UK Shale Oil Play. *In*: *SPE/EAGE European Unconventional Resources Conference and Exhibition* – SPE/EAGE

European Unconventional Resources Conference and Exhibition. Vienna, Austria, Society of Petroleum Engineers. https://doi.org/10.2118/150933-MS.

Selley, R.C. 2005. UK shale-gas resources. *In*: Dore, A.G. & Vining, B.A, (Eds.): *Petroleum Geology: North-West Europe and Global Perspectives – Proceedings of the 6th Petroleum Geology Conference.* Geological Society of London, 707–714. https://doi.org/10.1144/0060707.

Slowakiewicz, M., Tucker, M.E., Vane, C.H., Harding, R., Collins, A. & Pancost, R.D. 2015. Shale-gas potential of the mid-Carboniferous Bowland-Hodder unit in the Cleveland basin (Yorkshire), Central Britain. *Journal of Petroleum Geology*, **38**, 59–75. https://doi.org/10.1111/jpg.12598.

Smith, N., Turner, P. & Williams, G. 2010. UK data and analysis for shale gas prospectivity. *In*: Vining, B.A. & Pickering, S.C. (Eds.): *Petroleum Geology: From Mature Basins to New Frontiers—Proceedings of the 7th Petroleum Geology Conference*. Geological Society of London, 1087–1098. https://doi.org/10.1144/0071087.

Steele, R.P. 1988. The Namurian sedimentary history of the Gainsborough Trough. In: Besly, B.M. & Kelling, G. (eds) Sedimentation in a Syn-orogenic Basin Complex - the Upper Carboniferous of Northwest Europe. Blackie, Glasgow & London, 102-113.

Underhill, J.R. 2009. Role of intrusion-induced salt mobility in controlling the formation of the enigmatic "Silverpit Crater", UK Southern North Sea. Petroleum Geoscience, **15**, 197-216. https://doi.org/10.1144/1354-079309-843.

Underhill, J.R. 2018. Impact of Early Cenozoic Uplift and Exhumation for Unconventional Reserves in the Midland Valley Basin. Proceedings of the Open University Geological Society, **4**, 55-60.

Underhill, J.R., Gayer, R.A., Woodcock, N.H., Donnelly, R., Jolley, E.J. & Stimpson, I.G. 1988. The Dent Fault System, northern England—reinterpreted as a major oblique-slip fault zone. *Journal of the Geological Society*, **145**, 303–316. https://doi.org/10.1144/gsjgs.145.2.0303.

Underhill, J.R., Monaghan, A.A. & Browne, M.A.E. 2008. Controls on Structural Styles, Basin Development and Petroleum Prospectivity in the Midland Valley of Scotland. Marine and Petroleum Geology, 25, 1000-1022. https://doi.org/10.1016/j.marpetgeo.2007.12.002.

Walsh, J.J. & Watterson, J. 1988. Dips of normal faults in British Coal Measures and other sedimentary sequences. *Journal of the Geological Society*, **145**, 859-873. https://doi.org/10.1144/gsjgs.145.5.0859.

Watterson, J., Walsh, J.J., Gillespie, P.A. & Easton, S. 1996. Scaling systematics of fault sizes on a large-scale range fault map. *Journal of Structural Geology*, **18**, 199–214. https://doi.org/10.1016/S0191-8141(96)80045-9.

Westwood, R.F., Toon, S.M., Styles, P. & Cassidy, N.J. 2017. Horizontal respect distance for hydraulic fracturing in the vicinity of existing faults in deep geological reservoirs: a review and modelling study. *Geomechanics and Geophysics for Geo-Energy and Geo-Resources*, **3**, 379–391. https://doi.org/10.1007/s40948-017-0065-3.

Whitelaw, P., Uguna, C.N., Stevens, L.A., Meredith, W., Snape, C.E., Vane, C.H., Moss-Hayes, V. & Carr, A.D. 2019. Shale gas reserve evaluation by laboratory pyrolysis and gas holding capacity consistent with field data. Nature Communications, https://doi.org/10.1038/s41467-019-11653-4.

Wilson, A.A. 1990. The Mercia Mudstone Group (Trias) of the East Irish Sea Basin. *Proceedings of the Yorkshire Geological Society*, **48**, 1-22. https://doi.org/10.1144/pygs.48.1.1.

Worthington, R.P. & Walsh, J.J. 2011. Structure of Lower Carboniferous basins of NW Ireland, and its implications for structural inheritance and Cenozoic faulting. *Journal of Structural Geology*, **33**, 1285–1299. https://doi.org/10.1016/j.jsg.2011.05.001.

Yang, S., Horsfield, B., Mahlstedt, N., Stephenson, M. & Konitzer, S. 2015. On the primary and secondary petroleum generating characteristics of the Bowland Shale, Northern England. Journal of the Geological Society, 173, 292-305. https://doi.org/10.1144/jgs2015-056.

Yuan, G., Dwivedi, P., Kwok, C.K. & Malpani, R. 2017. The Impact of Increase in Lateral Length on Production Performance of Horizontal Shale Wells. *In*: *SPE Europec featured at 79th EAGE Conference and Exhibition.* Paris, France, Society of Petroleum Engineers, 15. https://doi.org/10.2118/185768-MS.

Figure Captions

Fig.1: Early Carboniferous structural elements of North England and Wales highlighting the key basins and platform areas (modified after Fraser *et al* (1990)). The gross tectonic setting was that of a series of blocks and basins formed by contemporaneous rifting. Mudstone-dominated sequences (Bowland Shale and equivalents) filled the basins, and extensive carbonate platforms developed on the blocks. The Ribblesdale Fold Belt and its' offshore counterpart (the Môn-Deemster Fold Belt) is also highlighted (after Pharoah *et al* (2019)).

Fig.2: Simplified bedrock lithostratigraphy, geological structure and key well penetrations within the Craven Basin and surrounding areas. Also shown is the location of Figure 4, which illustrates the outline of the 3D data volume used in this study. The figure draws upon British Geological Survey materials © UKRI 2019. BABH: Becconsall-

Ashnott buried high, BbF: Billsborrow Fault, Bc: Becconsall-1 well, Bk: Banks well, Bw: Boulsworth borehole, CA: Catlow Anticline, CFS: Clitheroe Fault System, CoA: Clitheroe Anticline, DF: Dent Fault, EF: Elswick Fault, GA: Gisburn Anticline, GF: Grimsargh Fault, HC: Holme Chapel well, Hk: Hesketh well, LbF: Larbeck Fault, NCF: North Craven Fault, OA: Oakenclough Fault, PF: Pendle Fault, PM: Pendle Monocline, Rw: Roddlesworth well, SA: Sykes Anticline, SbA: Slaidburn Anticline, SCF: South Craven Fault, SkA: Skipton Anticline, Sw: Swinden borehole, SwA: Swinden Anticline, TnA: Thornley Anticline, TtA Thornton Anticline, TtF: Thistleton Fault, WF: Woodsfold Fault, Wm: Whitmoor well.

Fig.3: Stratigraphic summary chart for the Carboniferous, Permian and Triassic sequences of north-west England. The Lower Carboniferous sediments that accumulated in deepwater basins (e.g. Craven Basin) are differentiated from those that are extensively developed on adjacent platforms (e.g. West Lancashire High). Also included are key marine bands that define the Carboniferous chronostratigraphy in the region, and seismic markers shown in the cross-sections presented in Figures 5-10.

Fig.4: Location map illustrating the extent of the seismic coverage, locations of key wells and cross-sections illustrated from within the Bowland-12 3D. Line of section C-C' intersects the PNR-1 well at the Base-Permian Unconformity and line of section D-D' intersects the PNR-1Z side-track at Bowland Shale level.

Fig.5: Correlation of seismic to well ties for the Grange Hill-1Z, Preese Hall-1 and PNR-1 wells. Acoustic impedance (AI) is plotted using wireline logs, transformed to reflection coefficients and convolved with a zero-phase, 30Hz Klauder wavelet to produce a synthetic trace equivalent to the seismic data volume to allow for direct comparison. Interpreted structural and stratigraphic relationships between the wells

are sketched with reference to an along-strike cross-section (Fig. 9). BG: Brennand Grit, Carb.: Carboniferous (undifferentiated), Ch: Collyhurst Sandstone Fm., GB: Greenhalgh Block, Ks: Kinderscout Grit Gp., LB: Lower Bowland Shale Fm., LC: Lower Coal Measures, MM: Manchester Marl Fm., PG: Pendle Grit, Rb: Roeburndale Fm., RR: Rough Rock, SS: Sabden Shale, US: Upper Shales.

Fig.6: NW-SE cross-section through the Bowland-12 survey tieing the Grange Hill-1Z and Elswick-1 wells along the main direction of structural dip. The section has also been extended to pass through Roseacre Wood, the proposed location of a shale gas drilling pad. The section is shown without interpretation (left) and with interpretation (right) to enable direct comparison between the data and our mapping. The main structural features and stratigraphic units are highlighted. Carb.: Carboniferous (undifferentiated), GB: Greenhalgh Block, PB: Poulton Block, SB: Singleton Block, WB: Weeton Block. Please refer to Fig. 5 for further acronyms used for the well-tops.

Fig.7: NW-SE cross-section through the Bowland-12 survey tieing the Preese Hall-1 and Thistleton-1 wells along the main direction of structural dip. The section is shown without interpretation (left) and with interpretation (right) for comparative purposes. The main structural features and stratigraphic units are highlighted. GB: Greenhalgh Block, PB: Poulton Block, SB: Singleton Block, TtF: Thistleton Fault, WB: Weeton Block. Please refer to Fig.5 for acronyms used for the well-tops.

Fig.8: NW-SE cross-section through the Bowland-12 survey tieing the PNR-1 well along the main direction of structural dip. The section is shown without interpretation (left) and with interpretation (right) for comparative purposes. The main structural features and stratigraphic units are highlighted. GB: Greenhalgh Block, WB: Weeton Block. Please refer to Fig.5 for acronyms used for the well-tops.

Fig.9: NNE-SSW cross-section through the Bowland-12 survey tieing the Grange Hill-1Z, Preese Hall-1 and PNR-1 wells along the main direction of structural strike. The section is shown without interpretation (left) and with interpretation (right) for comparative purposes. The main structural features and stratigraphic units are highlighted. GB: Greenhalgh Block, SB: Singleton Block, WB: Weeton Block. Please refer to Fig.5 for acronyms used for the well-tops.

Fig.10: N-S strike section illustrating the syn-sedimentary thickening of the Permo-Triassic section in the Elswick Graben. The section is shown without interpretation (left) and with interpretation (right) for comparative purposes. The occurrence of a major erosional sequence boundary, seismic facies and direct calibration by the Elswick-1 well all point to their being an additional Permian section beneath the classic Collyhurst Sandstone unit in the graben as a result of syn-sedimentary extensional fault activity. Please refer to Fig.5 for acronyms used for the well-tops.

Fig. 11: A timeslice extracted from the Bowland-12 survey at 600ms time which corresponds to the Base-Permian Unconformity in the centre of the survey, and intra Permo-Triassic in the west and east. The timeslice is shown without (upper) and with (lower) annotated major faults. The intersection with the Base-Permian Unconformity surface map is also highlighted. El-1: Elswick-1, GH-1Z: Grange Hill-1Z, PH-1: Preese Hall-1, RW: Roseacre Wood, Th-1: Thistleton-1.

Fig.12: A timeslice extracted from the Bowland-12 survey at 1200ms which is equivalent to the Lower Bowland Shale in the centre and the east of the survey. The timeslice is shown without interpretation (upper) and with interpretation (lower). The lower panel includes interpreted fault planes and the four fault-bounded compartments identified

within the footwall of the Thistleton Fault. The intersection with the Lower Bowland Shale surface map is also highlighted. Please refer to Fig. 11 for a list of well acronyms.

Fig.13: Time structure map for the Base Permian Unconformity across the Bowland-12 dataset showing the distribution of the extensional fault network that largely affects the south east of the survey and defines the course of the Elswick Graben. Well defined footwall highs lie to the west of the Thistleton and Elswick Faults. In the case of the latter, the fault-bound 3-way dip closure that hosts the Elswick gas field has been highlighted. The latter produced 1 Bcf of gas between 1996-2013 and while it is now depleted, it still constitutes a possible site for gas storage. Please refer to Fig. 11 for a list of well acronyms.

Fig.14: Time structure map for the Top of the Lower Bowland Shale. Mapping of three significant SW-NE reverse faults allow the area to the west of the (Permo-Triassic) Thistleton Fault to be subdivided into four main structural compartments. The identification of these structural subdomains places severe constraints on shale gas extraction. The Permo-Triassic normal faults that define the Elswick Graben overprint buried Carboniferous reverse faults and add structural complexity meaning shale gas exploration is maybe more challenged in this area. The line of section shown in Fig. 8 intersects the PNR-1 well at the Base-Permian Unconformity and the line of section shown in Fig. 9 intersects the PNR-1Z side-track at Bowland Shale level. Please refer to Fig. 11 for a list of well acronyms.

Fig.15: Schematic cross-sections oriented approximately NW-SE through the Craven Basin illustrating the key tectono-stratigraphic events that led to the development of the main structures affecting shale gas exploration in the area. (a): The Craven Basin is

established during a phase of Lower Carboniferous extension and is bound by the West Lancashire High and the Pennine High (off the section in the north-west). (b): Upper Carboniferous Variscan deformation results in the formation of reverse faults, structural inversion of pre-existing normal faults and the folding of Lower Carboniferous strata. This leads to the creation of significant paleo-topography. (c): The Variscan topography is eroded to produce the Base-Permian Unconformity (BPU) above which Permian-Triassic continental clastics are deposited. (d): Permian-Triassic extensional faulting leads to the creation of significant depocentres that overprint the Carboniferous structural configuration. While clearly important in its subsequent history of burial, the effects of Mesozoic subsidence and deposition and Cenozoic uplift, exhumation and local fault reactivation are not shown in order to emphasise the Late Paleozoic (Variscan) and Permo-Triassic evolution that created the main structures seen on the 3D seismic dataset. BABH: Becconsall-Ashnott Buried High, ElF: Elswick Fault, GB: Greenhalgh Block, HHF: Haves Ho Fault, LbF: Larbeck Fault, MHF: Moor Hey Fault, PB: Poulton Block, PF: Pendle Fault, SB: Singleton Block, SF: Summerer Fault, TtF: Thistleton Fault, WB: Weeton Block, WF: Woodsfold Fault, WLH: West Lancashire High.

Fig. 16: Schematic cartoon to illustrate the challenge and consequences for shale gas exploration drilling locations and wellbore pathways resulting from the fault patterns that affect the PEDL 165 license. (a) Dip map for the Lower Bowland Shale with fault overlays added in the SE area of the map. (b) A common risk segment map classified using the angle of dip and continuity of reflectors. Some measurements of maximum compartment widths based on the maximum stress orientations shown in (c) are provided. (c) A collection of maximum stress orientations including the mean orientation from the Sellafield boreholes (Kingdon *et al*, 2016) and the distribution of

orientations calculated at Grange Hill-1Z and Preese Hall-1 (Clarke *et al*, 2018). The average minimum horizontal stress of 80° shown was used in the production of map (b). (d) A schematic cartoon showing a plan view of a horizontal wellbore aligned with the minimum horizontal stress orientation showing zones of hydraulic fractures propagating in the direction of maximum horizontal stress. These diagrams serve to illustrate how bedding continuity, dip and faulting can be used to define ranked common risk segments and define, prioritise and rank the most preferential sites for unconventional drilling. When the orientation of the maximum horizontal compressive stress is introduced, it is possible use the optimal WSW-ENE drilling direction and the way in which the fault networks in the area to evaluate the position of well pads and the maximum length of a horizontal borehole pathway, which dictate the optimal drilling sites. Please refer to Fig. 11 for a list of well acronyms.

Table 1: Summary of the five key well sites (and two horizontal well side-tracks at Preston New Road (PNR)) that calibrate the interpretations described in this paper (see Fig. 4 for locations). The wells are ordered by date upon they reached TD (total depth).

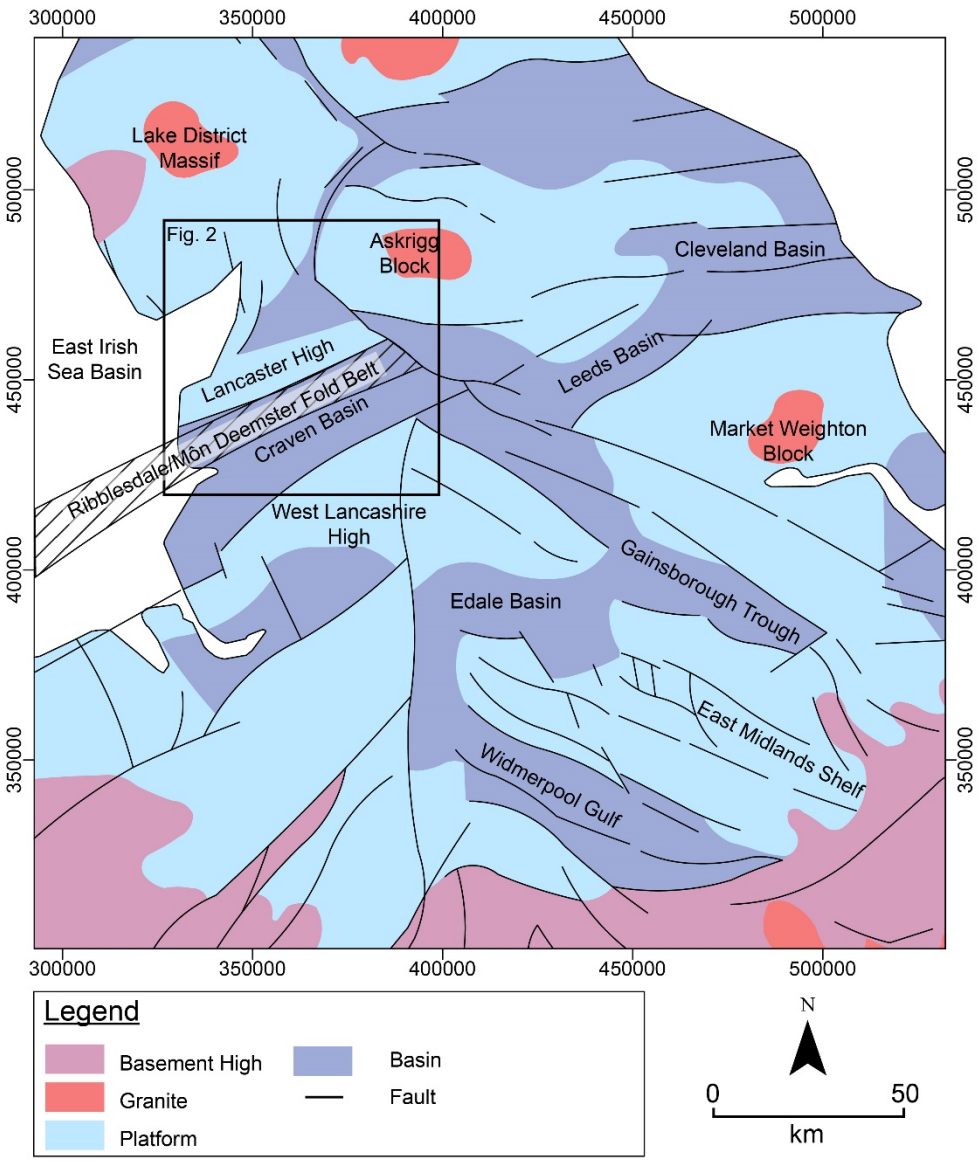
300000
350000
400000
450000
500000
Lake District Massif
Fig. 2
Askrigg Block
Cleveland Basin
East Irish Sea Basin
Lancaster High
Leeds Basin
Craven Basin
Ribblesdale/Mön Deemster Fold Belt
Market Weighton Block
West Lancashire High
Gainsborough Trough
Edale Basin
East Midlands Shelf
Widmerpool Gulf
Legend
Basement High
Granite
Platform
Basin
Fault
N
0
50
km

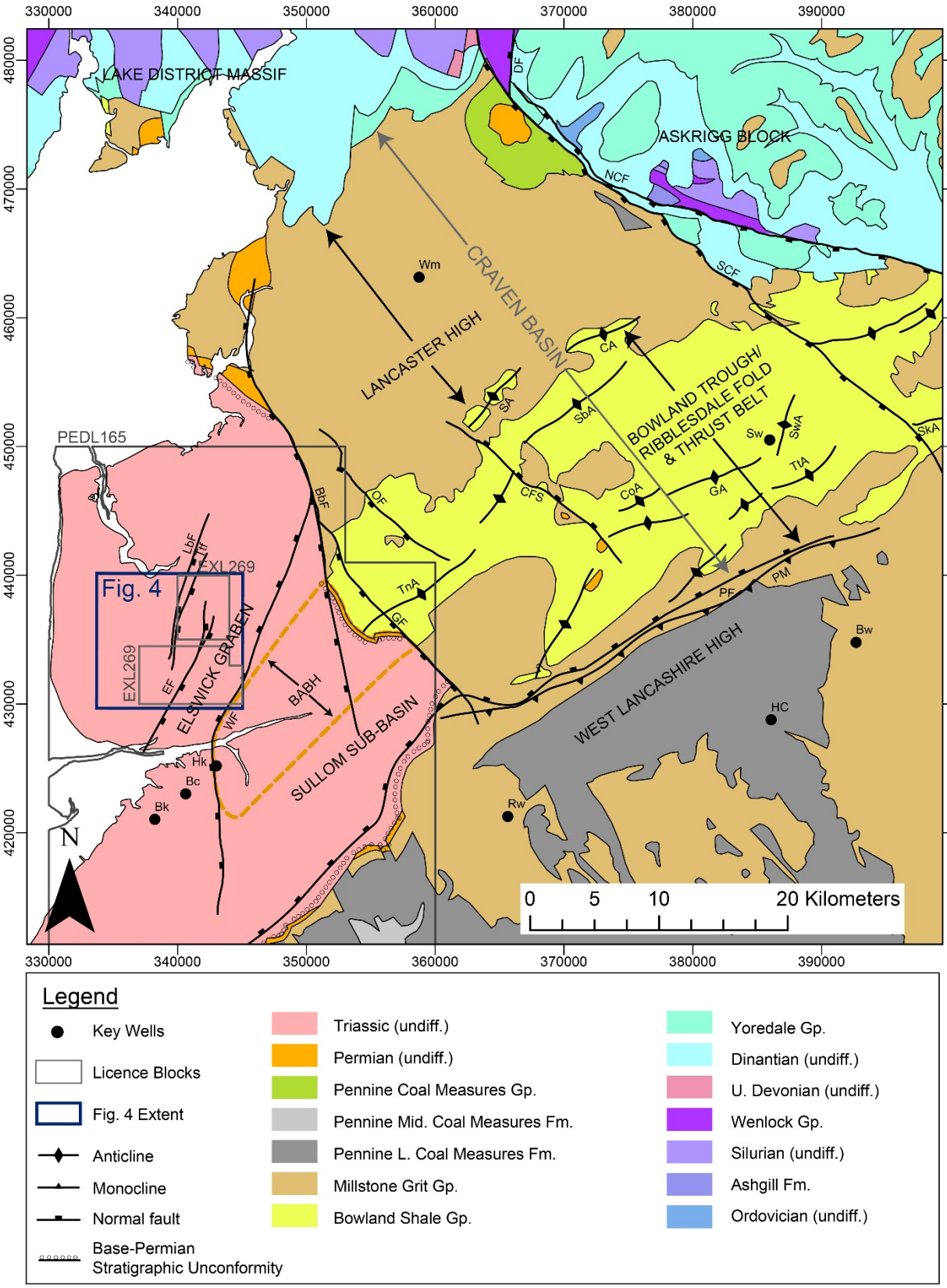
330000
340000
350000
360000
370000
380000
390000
480000
470000
460000
450000
440000
430000
420000
LAKE DISTRICT MASSIF
ASKRIGG BLOCK
CRAVEN BASIN
LANCASTER HIGH
BOWLAND TROUGH/
RIBBLESDALE FOLD
& THRUST BELT
WEST LANCASHIRE HIGH
ELSWICK GRABEN
SULLOM SUB-BASIN
PEDL165
EXL269
Fig. 4
DF
NCF
SCF
BbF
OF
CFS
CA
SA
SbA
CoA
GA
SwA
SkA
TlA
TnA
GF
PF
PM
LbF
TF
EF
WF
BABH
Wm
Sw
Bw
HC
Rw
Hk
Bc
Bk
N
0
5
10
20 Kilometers
Legend
Key Wells
Licence Blocks
Fig. 4 Extent
Anticline
Monocline
Normal fault
Base-Permian
Stratigraphic Unconformity
Triassic (undiff.)
Permian (undiff.)
Pennine Coal Measures Gp.
Pennine Mid. Coal Measures Fm.
Pennine L. Coal Measures Fm.
Millstone Grit Gp.
Bowland Shale Gp.
Yoredale Gp.
Dinantian (undiff.)
U. Devonian (undiff.)
Wenlock Gp.
Silurian (undiff.)
Ashgill Fm.
Ordovician (undiff.)

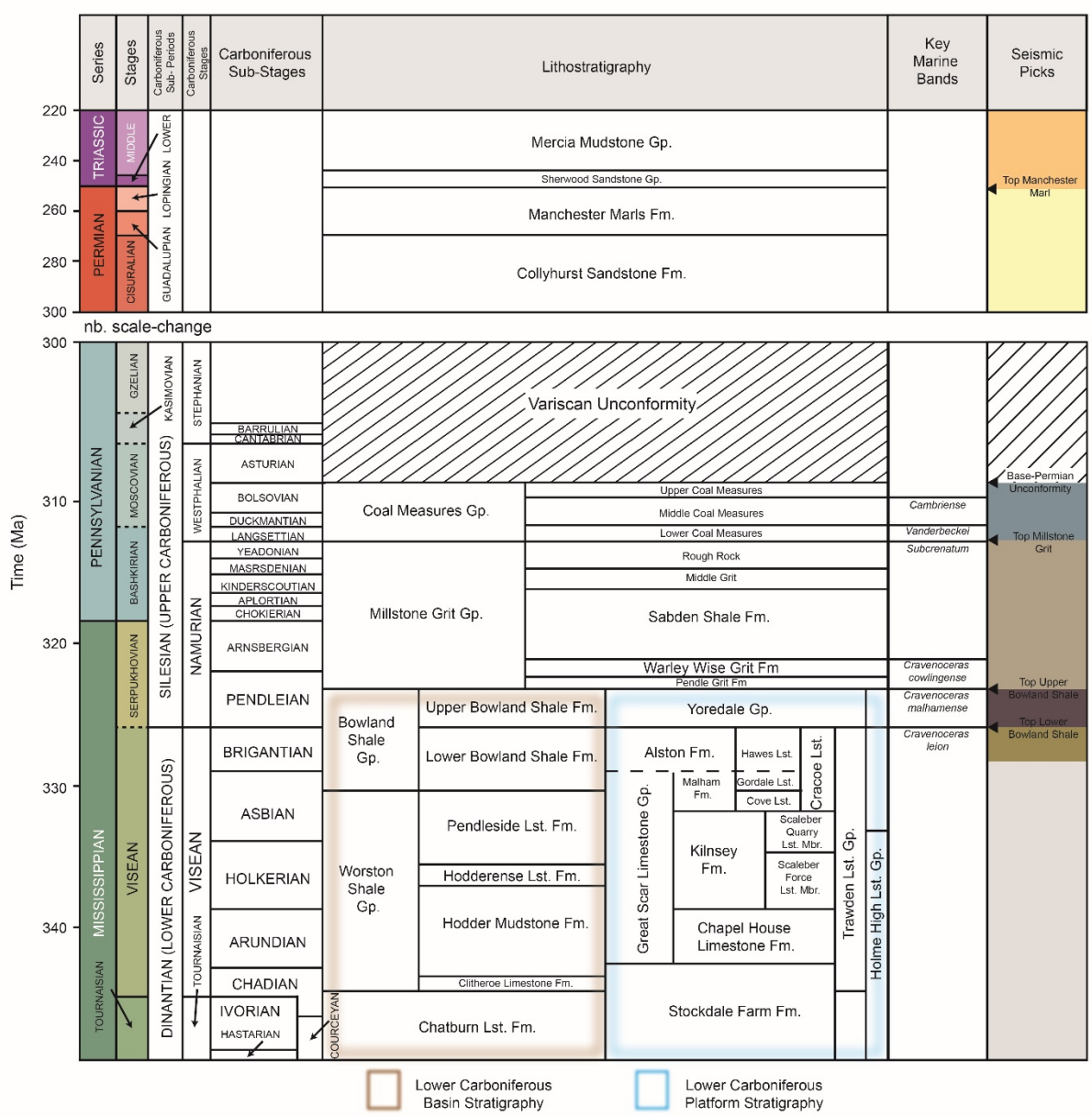
Series
Stages
Carboniferous Sub- Periods
Carboniferous Stages
Carboniferous Sub-Stages
Lithostratigraphy
Key Marine Bands
Seismic Picks
Time (Ma)
TRIASSIC
PERMIAN
MIDDLE
LOWER
LOPINGIAN
GUADALUPIAN
CISURALIAN
Mercia Mudstone Gp.
Sherwood Sandstone Gp.
Manchester Marls Fm.
Collyhurst Sandstone Fm.
Top Manchester Marl
nb. scale-change
PENNSYLVANIAN
MISSISSIPPIAN
GZELIAN
MOSCOVIAN
BASHKIRIAN
SERPUKHOVIAN
TOURNAISIAN
KASIMOVIAN
SILESIAN (UPPER CARBONIFEROUS)
DINANTIAN (LOWER CARBONIFEROUS)
NAMURIAN
VISEAN
TOURNAISIAN
STEPHANIAN
WESTPHALIAN
BARRUILIAN
CANTABRIAN
ASTURIAN
BOLSOVIAN
DUCKMANTIAN
LANGSETTIAN
YEADONIAN
MASRSDENIAN
KINDERSCOUTIAN
APLORTIAN
CHOKIERIAN
ARNSBERGIAN
PENDLEIAN
BRIGANTIAN
ASBIAN
HOLKERIAN
ARUNDIAN
CHADIAN
IVORIAN
HASTARIAN
COURCEYAN
Variscan Unconformity
Coal Measures Gp.
Upper Coal Measures
Middle Coal Measures
Lower Coal Measures
Millstone Grit Gp.
Rough Rock
Middle Grit
Sabden Shale Fm.
Warley Wise Grit Fm
Pendle Grit Fm
Bowland Shale Gp.
Upper Bowland Shale Fm.
Lower Bowland Shale Fm.
Worston Shale Gp.
Pendleside Lst. Fm.
Hodderense Lst. Fm.
Hodder Mudstone Fm.
Clitheroe Limestone Fm.
Chatburn Lst. Fm.
Yoredale Gp.
Alston Fm.
Hawes Lst.
Malham Fm.
Gordale Lst.
Cove Lst.
Cracoe Lst.
Great Scar Limestone Gp.
Kilnsey Fm.
Scaleber Quarry Lst. Mbr.
Scaleber Force Lst. Mbr.
Chapel House Limestone Fm.
Stockdale Farm Fm.
Trawden Lst. Gp.
Holme High Lst. Gp.
Cambriense
Vanderbeckei
Subcrenatum
Cravenoceras cowlingense
Cravenoceras malhamense
Cravenoceras leion
Base-Permian Unconformity
Top Millstone Grit
Top Upper Bowland Shale
Top Lower Bowland Shale
Lower Carboniferous Basin Stratigraphy
Lower Carboniferous Platform Stratigraphy

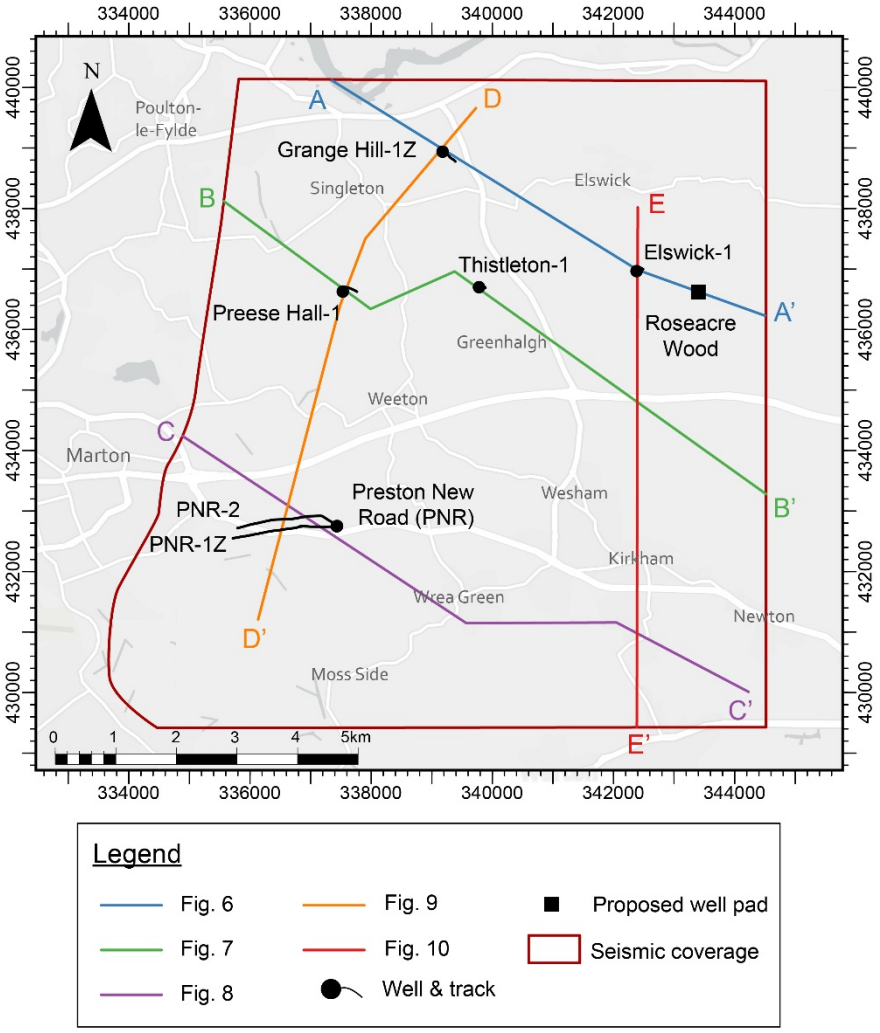
334000
336000
338000
340000
342000
344000
440000
438000
436000
434000
432000
430000
N
Poulton-
le-Fylde
A
D
Grange Hill-1Z
Singleton
Elswick
B
E
Elswick-1
Thistleton-1
A'
Preese Hall-1
Roseacre
Wood
Greenhalgh
Weeton
C
Marton
Preston New
Road (PNR)
Wesham
B'
PNR-2
PNR-1Z
Kirkham
Wrea Green
Newton
D'
Moss Side
C'
E'
0
1
2
3
4
5km
Legend
Fig. 6
Fig. 7
Fig. 8
Fig. 9
Fig. 10
Well & track
Proposed well pad
Seismic coverage

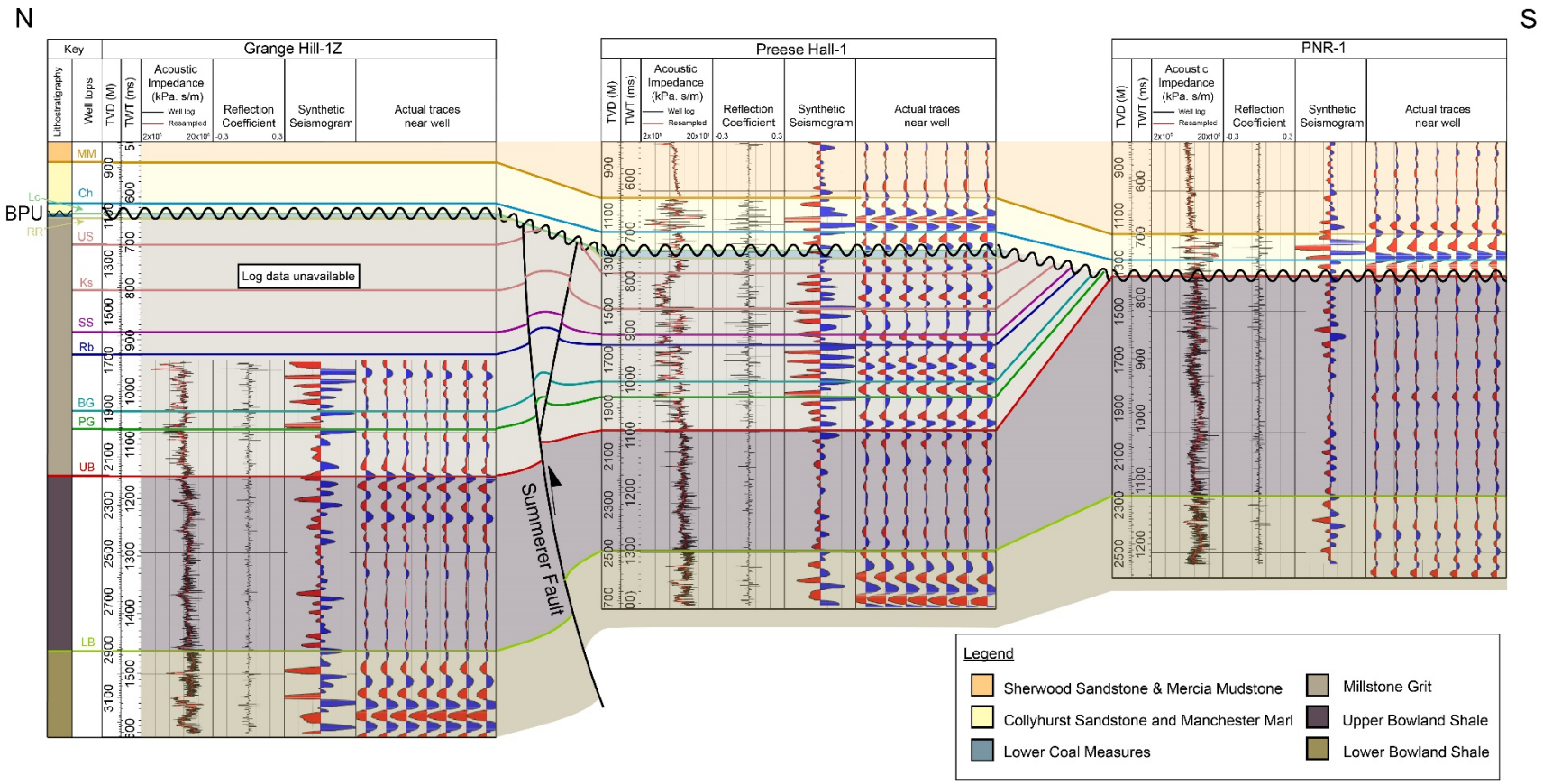
N
S
Key
Grange Hill-1Z
Preese Hall-1
PNR-1
Lithostratigraphy
Well tops
TVD (M)
TWT (ms)
Acoustic Impedance (kPa. s/m)
Well log
Resampled
Reflection Coefficient
Synthetic Seismogram
Actual traces near well
MM
Ch
Lc
BPU
RR
US
Ks
SS
Rb
BG
PG
UB
LB
Log data unavailable
Summerer Fault
Legend
Sherwood Sandstone & Mercia Mudstone
Collyhurst Sandstone and Manchester Marl
Lower Coal Measures
Millstone Grit
Upper Bowland Shale
Lower Bowland Shale

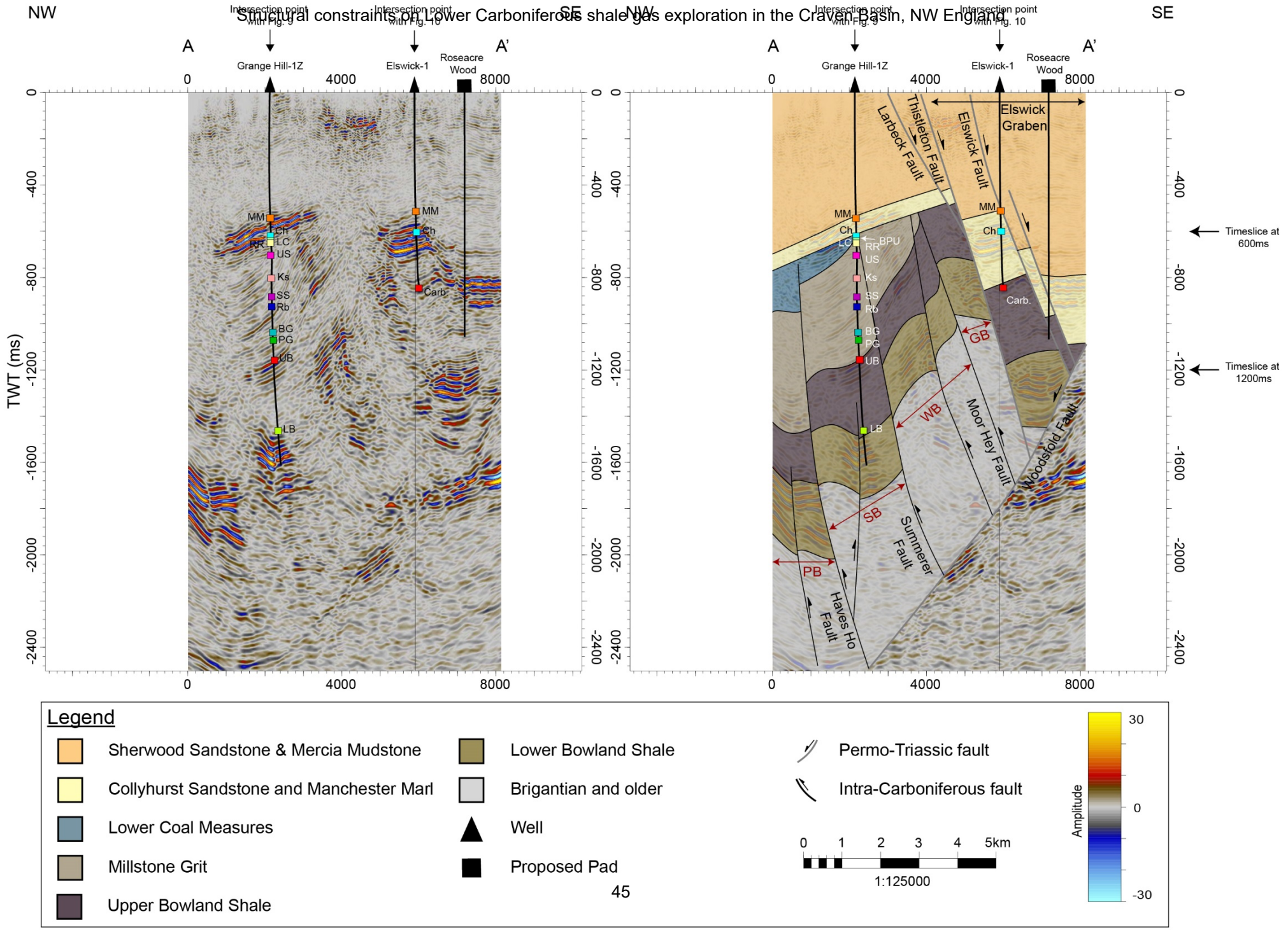
NW
SE
NW
SE
A
A'
Intersection point with Fig. 9
Intersection point with Fig. 10
Grange Hill-1Z
Elswick-1
Roseacre Wood
0
4000
8000
TWT (ms)
0
-400
-800
-1200
-1600
-2000
-2400
MM
Ch
LC
RR
US
Ks
SS
Rb
BG
PG
UB
LB
Carb.
BPU
Larbeck Fault
Thistleton Fault
Elswick Fault
Elswick Graben
GB
WB
SB
PB
Moor Hey Fault
Woodsfold Fault
Summerer Fault
Haves Ho Fault
Timeslice at 600ms
Timeslice at 1200ms
Legend
Sherwood Sandstone & Mercia Mudstone
Collyhurst Sandstone and Manchester Marl
Lower Coal Measures
Millstone Grit
Upper Bowland Shale
Lower Bowland Shale
Brigantian and older
Well
Proposed Pad
Permo-Triassic fault
Intra-Carboniferous fault
0 1 2 3 4 5km
1:125000
Amplitude
30
0
-30

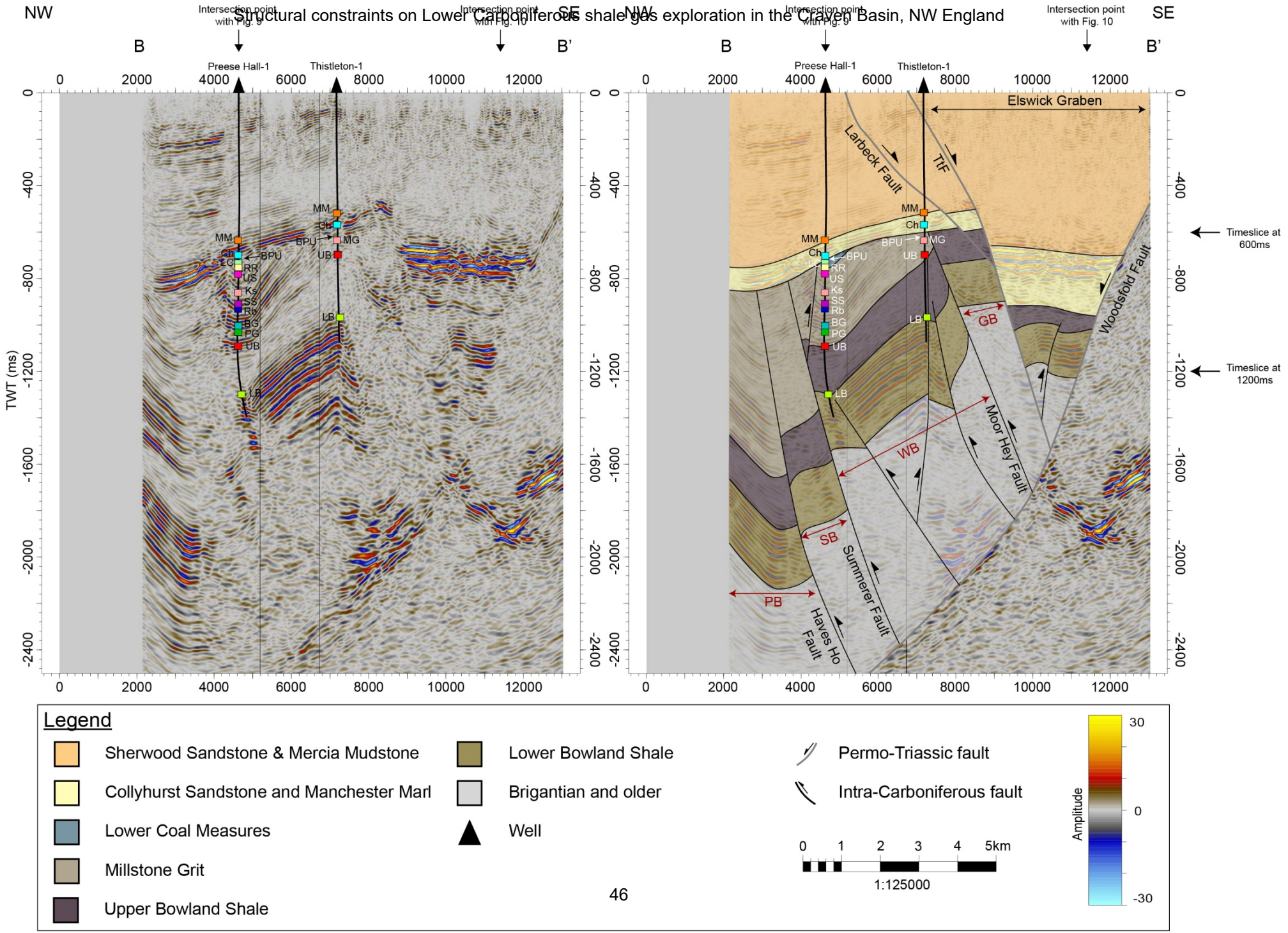
NW
SE
B
B'
Intersection point with Fig. 9
Intersection point with Fig. 10
Preese Hall-1
Thistleton-1
TWT (ms)
MM
Ch
BPU
MG
UB
LB
RR
US
Ks
SS
Rb
BG
PG
Elswick Graben
Larbeck Fault
TfF
Woodsfold Fault
Moor Hey Fault
Summerer Fault
Haves Ho Fault
GB
WB
SB
PB
Timeslice at 600ms
Timeslice at 1200ms
Legend
Sherwood Sandstone & Mercia Mudstone
Collyhurst Sandstone and Manchester Marl
Lower Coal Measures
Millstone Grit
Upper Bowland Shale
Lower Bowland Shale
Brigantian and older
Well
Permo-Triassic fault
Intra-Carboniferous fault
0 1 2 3 4 5km
1:125000
Amplitude
30
0
-30

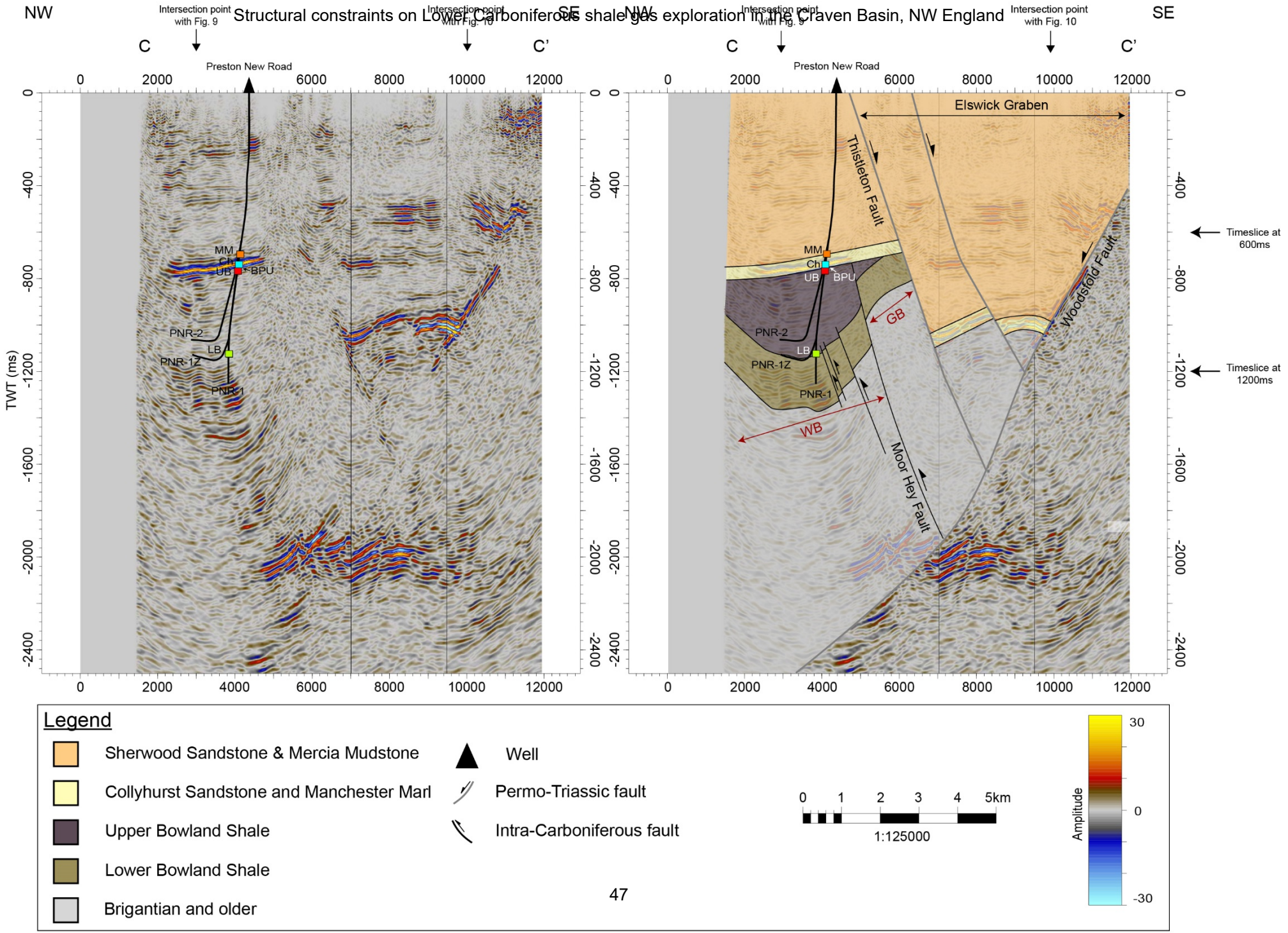
NW
SE
NW
SE
Intersection point with Fig. 9
Intersection point with Fig. 10
Intersection point with Fig. 9
Intersection point with Fig. 10
C
C'
C
C'
Preston New Road
Preston New Road
TWT (ms)
MM
Ch
UB
BPU
PNR-2
LB
PNR-1Z
PNR-1
Elswick Graben
Thistleton Fault
Woodsfold Fault
Moor Hey Fault
GB
WB
Timeslice at 600ms
Timeslice at 1200ms
Legend
Sherwood Sandstone & Mercia Mudstone
Collyhurst Sandstone and Manchester Marl
Upper Bowland Shale
Lower Bowland Shale
Brigantian and older
Well
Permo-Triassic fault
Intra-Carboniferous fault
0 1 2 3 4 5km
1:125000
Amplitude
30
0
-30

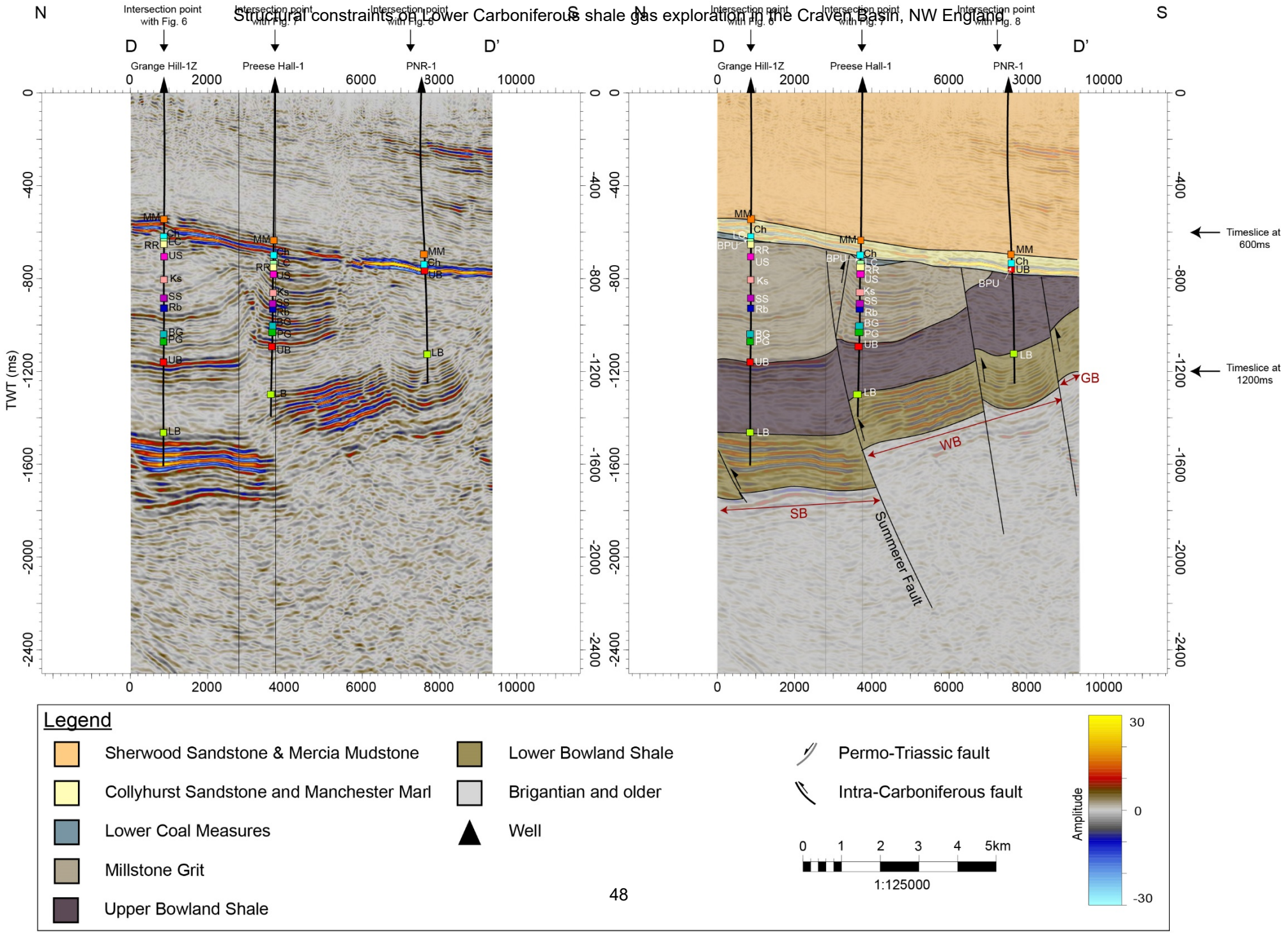
N
S
D
D'
Intersection point with Fig. 6
Intersection point with Fig. 7
Intersection point with Fig. 8
Grange Hill-1Z
Preese Hall-1
PNR-1
TWT (ms)
MM
Ch
LC
RR
US
Ks
SS
Rb
BG
PG
UB
LB
BPU
GB
WB
SB
Summerer Fault
Timeslice at 600ms
Timeslice at 1200ms
Legend
Sherwood Sandstone & Mercia Mudstone
Collyhurst Sandstone and Manchester Marl
Lower Coal Measures
Millstone Grit
Upper Bowland Shale
Lower Bowland Shale
Brigantian and older
Well
Permo-Triassic fault
Intra-Carboniferous fault
0 1 2 3 4 5km
1:125000
Amplitude
30
0
-30

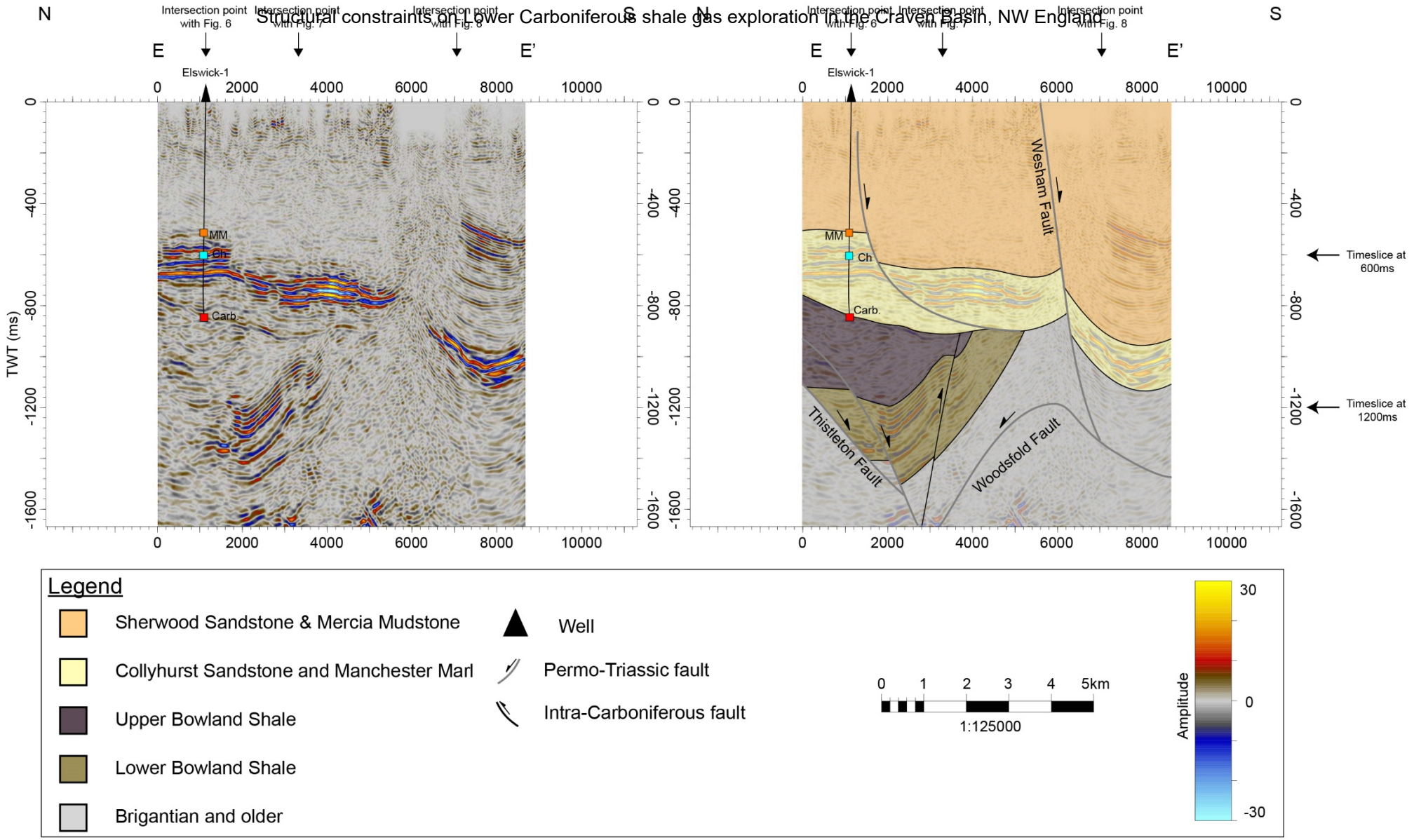
N
S
N
S
Intersection point with Fig. 6
Intersection point with Fig. 7
Intersection point with Fig. 8
E
E'
Elswick-1
MM
Ch
Carb.
TWT (ms)
Wesham Fault
Thistleton Fault
Woodsfold Fault
Timeslice at 600ms
Timeslice at 1200ms
Legend
Sherwood Sandstone & Mercia Mudstone
Collyhurst Sandstone and Manchester Marl
Upper Bowland Shale
Lower Bowland Shale
Brigantian and older
Well
Permo-Triassic fault
Intra-Carboniferous fault
0 1 2 3 4 5km
1:125000
Amplitude
30
0
-30

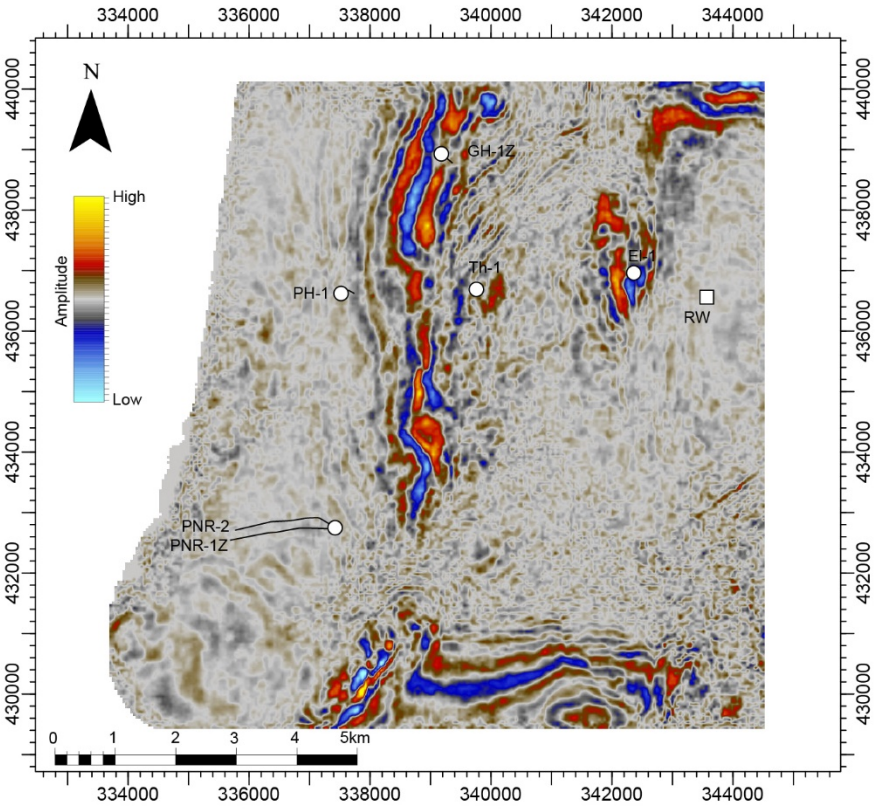
334000
336000
338000
340000
342000
344000
440000
438000
436000
434000
432000
430000
N
High
Amplitude
Low
GH-1Z
PH-1
Th-1
El-1
RW
PNR-2
PNR-1Z
0
1
2
3
4
5km

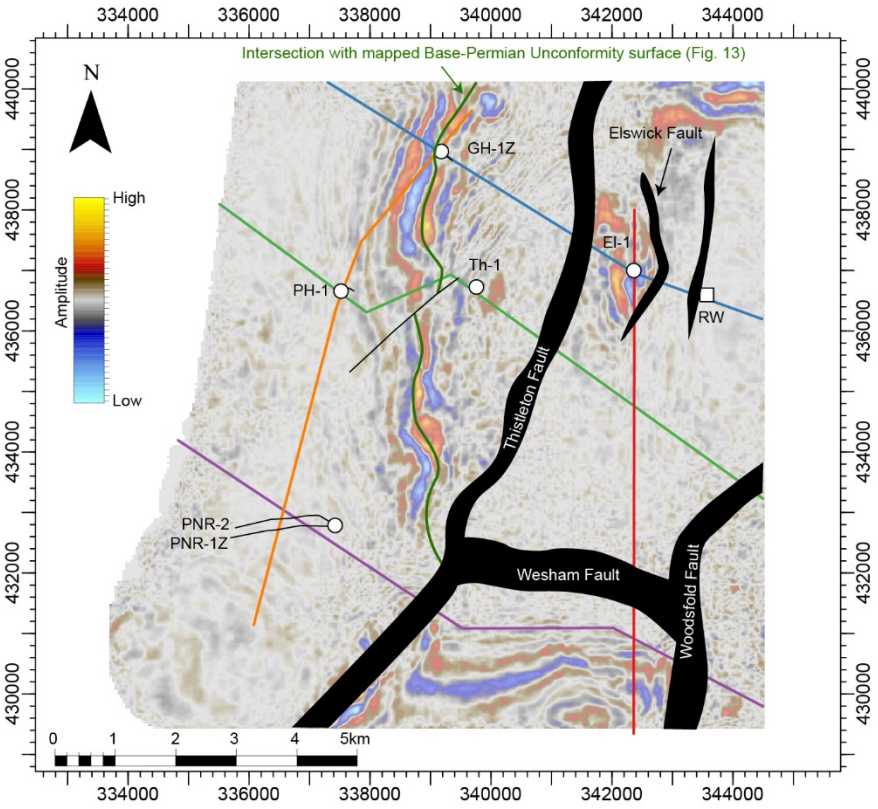
Intersection with mapped Base-Permian Unconformity surface (Fig. 13)
334000
336000
338000
340000
342000
344000
440000
438000
436000
434000
432000
430000
N
High
Amplitude
Low
GH-1Z
Elswick Fault
El-1
Th-1
PH-1
RW
Thistleton Fault
PNR-2
PNR-1Z
Wesham Fault
Woodsfold Fault
0
1
2
3
4
5km

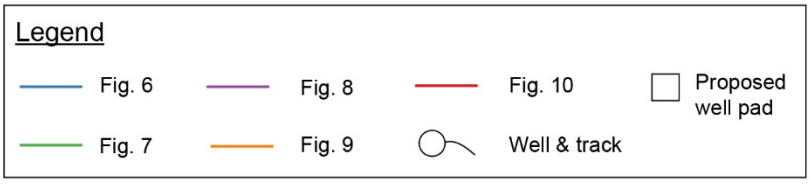
Legend
Fig. 6
Fig. 8
Fig. 10
Proposed well pad
Fig. 7
Fig. 9
Well & track

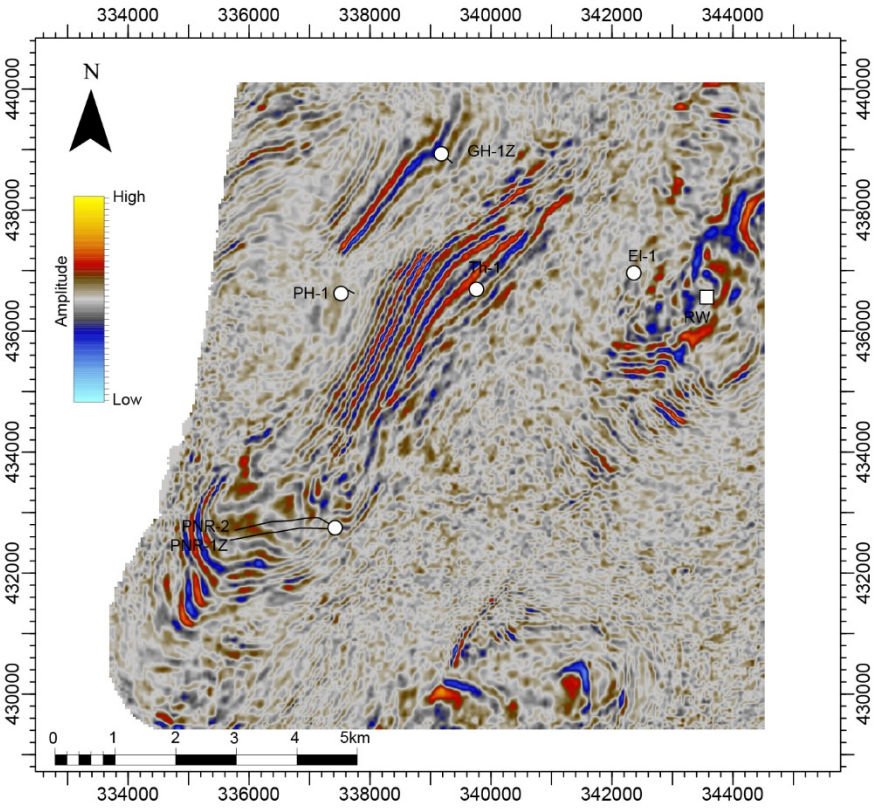
334000
336000
338000
340000
342000
344000
440000
438000
436000
434000
432000
430000
N
High
Amplitude
Low
GH-1Z
PH-1
Th-1
EI-1
RW
PNR-2
PNR-1Z
0
1
2
3
4
5km

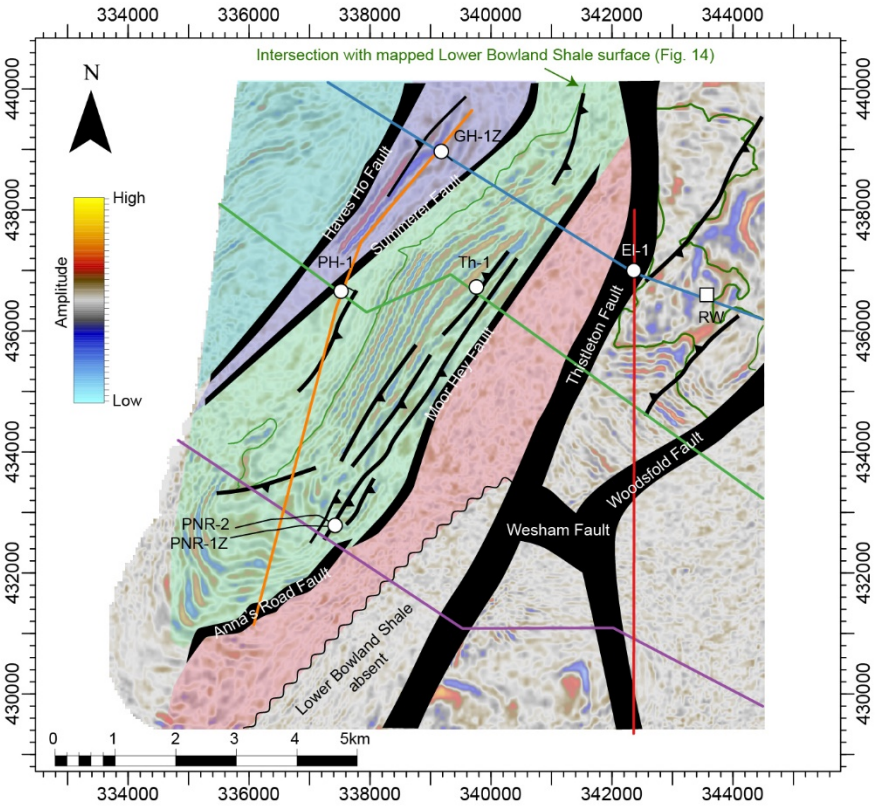
Intersection with mapped Lower Bowland Shale surface (Fig. 14)
N
High
Amplitude
Low
GH-1Z
Hawes HG Fault
Summerseat Fault
PH-1
Th-1
EI-1
RW
Thistleton Fault
Moon Hey Fault
Woodsfold Fault
Wesham Fault
PNR-2
PNR-1Z
Anna's Road Fault
Lower Bowland Shale absent
0
1
2
3
4
5km


Legend
Poulton Block
Greenhalgh Block
Fig. 8
Well & track
Singleton Block
Fig. 6
Fig. 9
Proposed well pad
Weeton Block
Fig. 7
Fig. 10

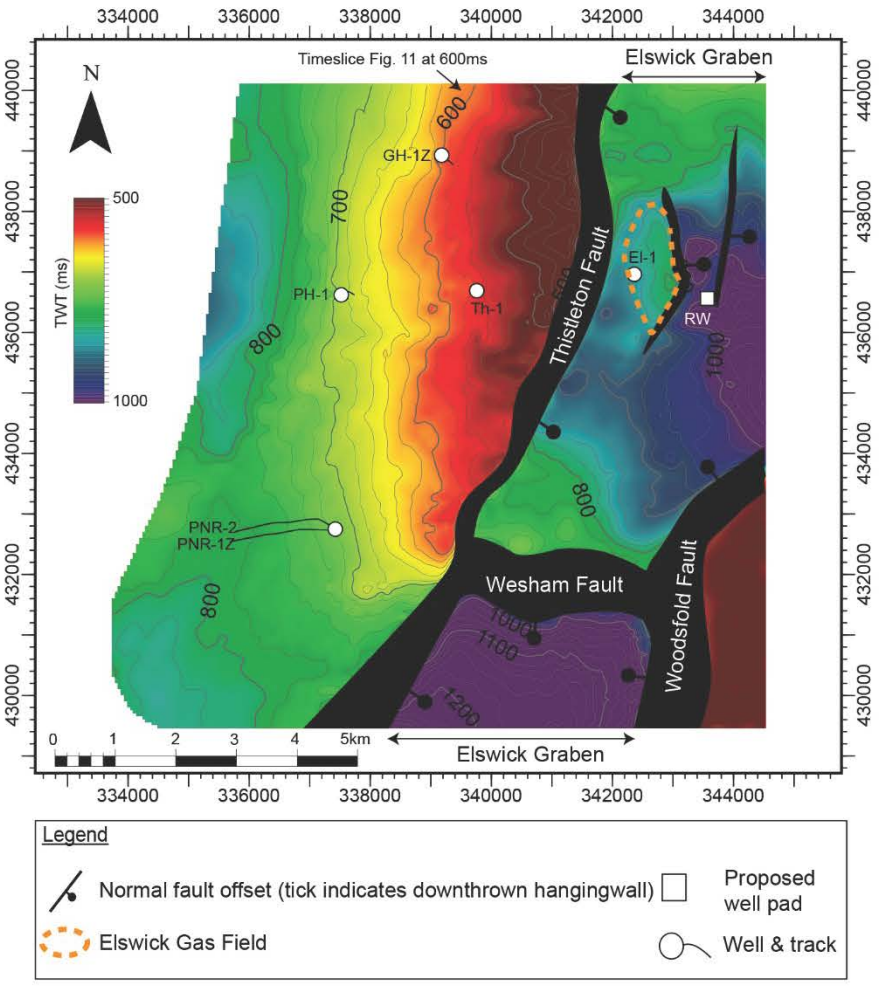
334000
336000
338000
340000
342000
344000
440000
438000
436000
434000
432000
430000
N
Timeslice Fig. 11 at 600ms
Elswick Graben
TWT (ms)
500
1000
600
700
800
GH-1Z
PH-1
Th-1
PNR-2
PNR-1Z
Thistleton Fault
EI-1
RW
Wesham Fault
Woodsfold Fault
1000
1100
1200
0
1
2
3
4
5km
Elswick Graben
Legend
Normal fault offset (tick indicates downthrown hangingwall)
Proposed well pad
Elswick Gas Field
Well & track

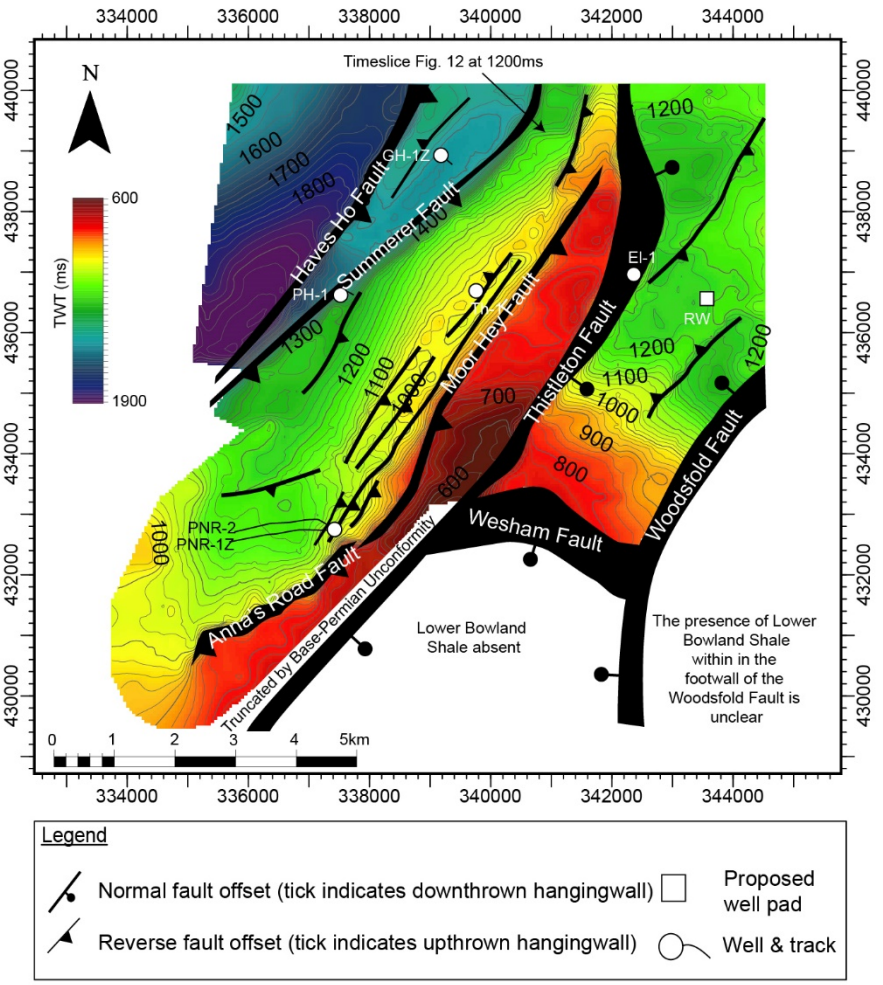
334000
336000
338000
340000
342000
344000
440000
438000
436000
434000
432000
430000
N
Timeslice Fig. 12 at 1200ms
TWT (ms)
600
1900
1500
1600
1700
1800
1400
1300
1200
1100
1000
900
800
700
600
1000
1200
GH-1Z
PH-1
EI-1
RW
Haves Ho Fault
Summerer Fault
Moor Hey Fault
Thistleton Fault
Woodsfold Fault
Wesham Fault
Anna's Road Fault
PNR-2
PNR-1Z
Truncated by Base-Permian Unconformity
Lower Bowland Shale absent
The presence of Lower Bowland Shale within in the footwall of the Woodsfold Fault is unclear
0
1
2
3
4
5km
Legend
Normal fault offset (tick indicates downthrown hangingwall)
Reverse fault offset (tick indicates upthrown hangingwall)
Proposed well pad
Well & track

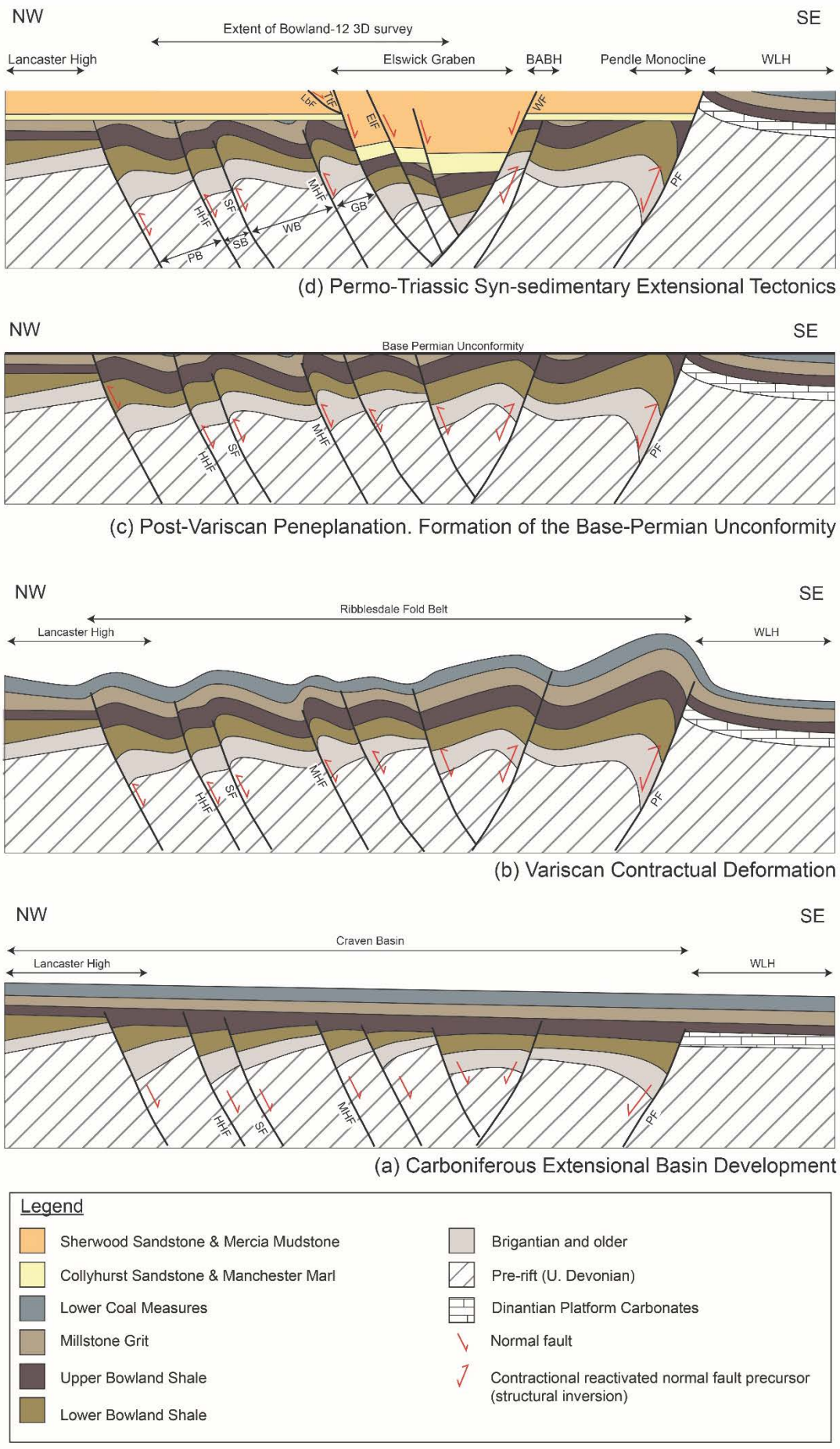
NW
SE
Extent of Bowland-12 3D survey
Lancaster High
Elswick Graben
BABH
Pendle Monocline
WLH
LDF
TFF
EIF
WF
PF
MHF
GB
HHF
SF
WB
SB
PB
(d) Permo-Triassic Syn-sedimentary Extensional Tectonics
NW
SE
Base Permian Unconformity
HHF
SF
MHF
PF
(c) Post-Variscan Peneplanation. Formation of the Base-Permian Unconformity
NW
SE
Ribblesdale Fold Belt
Lancaster High
WLH
HHF
SF
MHF
PF
(b) Variscan Contractual Deformation
NW
SE
Craven Basin
Lancaster High
WLH
HHF
SF
MHF
PF
(a) Carboniferous Extensional Basin Development
Legend
Sherwood Sandstone & Mercia Mudstone
Collyhurst Sandstone & Manchester Marl
Lower Coal Measures
Millstone Grit
Upper Bowland Shale
Lower Bowland Shale
Brigantian and older
Pre-rift (U. Devonian)
Dinantian Platform Carbonates
Normal fault
Contractional reactivated normal fault precursor (structural inversion)

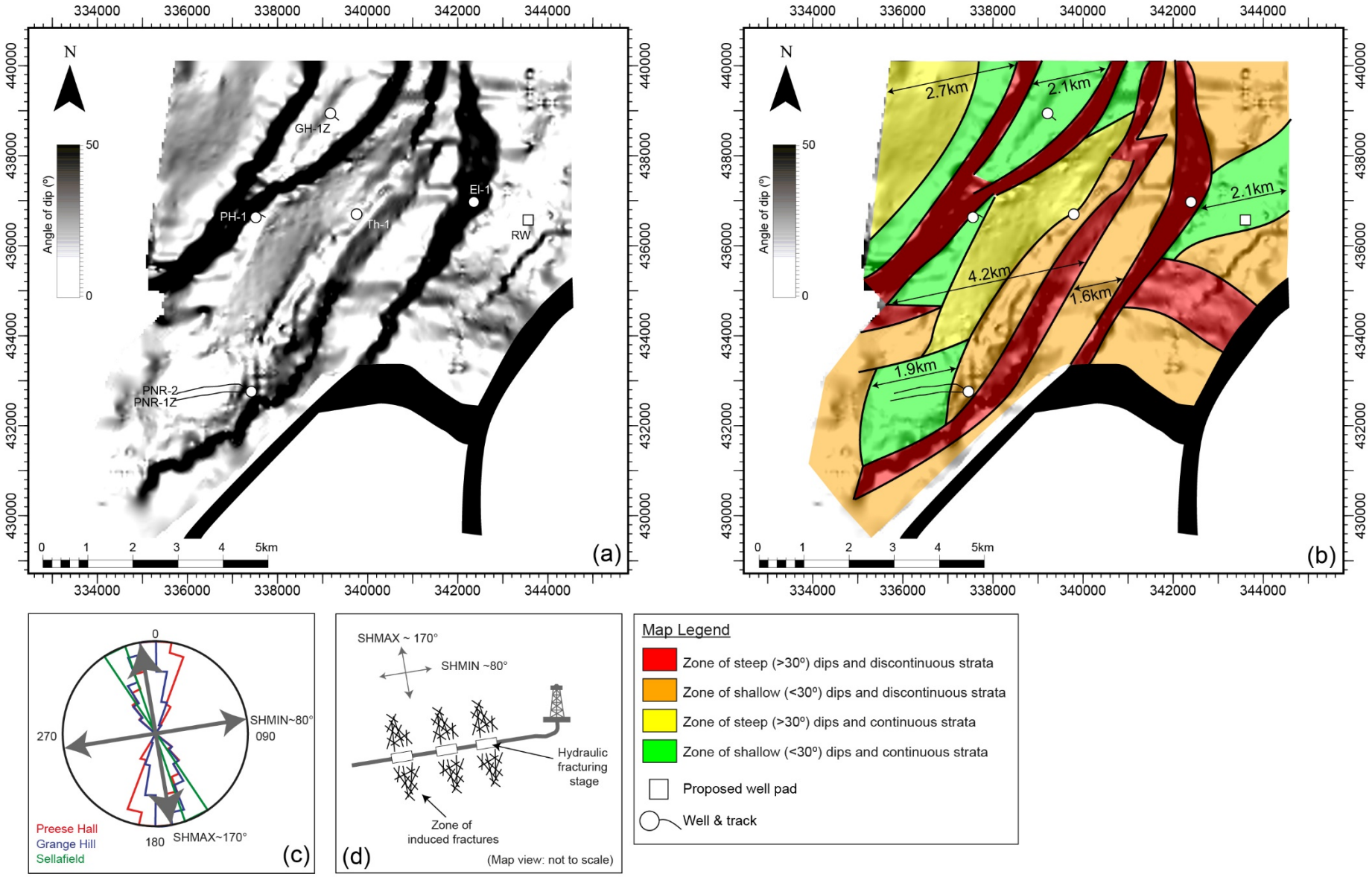
334000
336000
338000
340000
342000
344000
440000
438000
436000
434000
432000
430000
N
Angle of dip (°)
50
0
GH-1Z
PH-1
Th-1
EI-1
RW
PNR-2
PNR-1Z
0 1 2 3 4 5km
(a)
2.7km
2.1km
2.1km
4.2km
1.6km
1.9km
(b)
0
SHMIN~80°
090
270
180
SHMAX~170°
Preese Hall
Grange Hill
Sellafield
(c)
SHMAX ~ 170°
SHMIN ~80°
Hydraulic fracturing stage
Zone of induced fractures
(d)
(Map view: not to scale)
Map Legend
Zone of steep (>30°) dips and discontinuous strata
Zone of shallow (<30°) dips and discontinuous strata
Zone of steep (>30°) dips and continuous strata
Zone of shallow (<30°) dips and continuous strata
Proposed well pad
Well & track

Name	Operator	Date Spudded	Date TD'd	Type	TD (m)	TD (stratigraphy)	Additional Notes
Thistleton-1	British Gas	23/12/1987	11/02/1988	Conventional	2140	L. Bowland Shale	Exploration well with Permo-Triassic (Collyhurst Sandstone) target. Plugged and Abandoned as a dry hole.
Elswick-1	British Gas	29/04/1990	24/05/1990	Conventional	1615	Carboniferous (undifferentiated)	Permo-Triassic gas discovery. Produced 1 Bcf of gas between 1996 and 2013. Production license operatorship transferred to Warwick Resources
Preese Hall-1	Cuadrilla Resources	16/08/2010	04/12/2010	Unconventional	2774	L. Bowland Shale	Vertical shale-gas evaluation well. Six hydraulic fracture treatments carried out and induced seismicity recorded up to 2.3M_L.
Grange Hill-1Z	Cuadrilla Resources	15/01/2011	20/07/2011	Unconventional	3284	L. Bowland Shale	Vertical shale-gas evaluation well.
Preston New Road-1 (PNR-1)	Cuadrilla Resources	16/09/2017	02/01/2018	Unconventional	2712	L. Bowland Shale	Vertical shale-gas evaluation well.
PNR-1Z	Cuadrilla Resources	11/01/2018 (kick-off date)	21/03/2018	Unconventional	3424	L. Bowland Shale	782m lateral section within the Lower Bowland Shale. Hydraulic fracture treatments carried out at 15 stages with induced seismicity recorded up to 1.5M_L.
PNR-2	Cuadrilla Resources	17/08/2018	04/07/2018	Unconventional	3163	U. Bowland Shale	744m lateral section within the U. Bowland Shale. Hydraulic fracture treatments carried out in 2019 and induced seismicity recorded up to 2.9M_L.